

Clemson University

TigerPrints

All Theses

Theses

12-2022

Flexural Bond Strength of Masonry Assemblies with Lightweight Grout

Benjamin L. Hiner

Clemson University, bhiner@clemson.edu

Follow this and additional works at: https://tigerprints.clemson.edu/all_theses



Part of the [Civil Engineering Commons](#), and the [Structural Engineering Commons](#)

Recommended Citation

Hiner, Benjamin L., "Flexural Bond Strength of Masonry Assemblies with Lightweight Grout" (2022). *All Theses*. 3937.

https://tigerprints.clemson.edu/all_theses/3937

This Thesis is brought to you for free and open access by the Theses at TigerPrints. It has been accepted for inclusion in All Theses by an authorized administrator of TigerPrints. For more information, please contact kokeefe@clemson.edu.

FLEXURAL BOND STRENGTH OF MASONRY ASSEMBLIES WITH LIGHTWEIGHT GROUT

A Thesis

Presented to

The Graduate School of
Clemson University

In Partial Fulfillment

of the Requirements for the Degree
Master of Engineering

by

Ben Hiner

December 2022

Accepted By:

Dr. Laura Redmond, Committee Chair

Dr. M. Z. Naser

Dr. Michael Stoner

ABSTRACT

Lightweight grout has many potential benefits in masonry construction, including minimizing mass, improving thermal performance, and potentially reducing shrinkage cracking via internal curing. However, insufficient testing of masonry assemblies with lightweight grout has been conducted to suggest appropriate design modification factors akin to the lambda factor in ACI 318-19. The objective of this paper is to study the tensile bond behavior of masonry assemblies grouted with lightweight grout and to suggest appropriate equations for predicting design capacity. A moment couple test is designed specifically for grouted masonry assemblies and has additional capacity compared to the traditional ASTM 1072 bond wrench device. In this type of test, expanded clay aggregates are used to formulate a grout mix used to form two-unit fully grouted masonry assemblies for the testing. This thesis discusses the design of the moment couple test device, the preparation of the grouted prisms used to test flexural bond strength, and the results of the flexural bond strength testing. The results of the testing indicate that the current tabulated values for fully grouted masonry subjected to tension normal to the bed joint may be sufficiently conservative for use with assemblies comprised of lightweight grout. Future research will include the testing of masonry assemblies constructed with expanded slate masonry grout and will examine the relationship between the flexural tensile strength and the equilibrium density of the grout.

Keywords: Lightweight, Grout, Normal-weight, Concrete, Masonry, Bond Strength, Compression Strength

DEDICATION

I would like to dedicate this paper to my parents: Rick and Amanda Hiner, and to my brothers Andrew and Caleb. I never would have been able to make it through this entire process without your love and support. Thank you for always believing in me and helping me in any way you could. I love you all so much!

ACKNOWLEDGEMENT

I would like to thank Dr. Laura Redmond for choosing me for this project and for dedicating so much time to helping and guiding me through it. I had very much enjoyed her classes during my undergraduate degree and was very grateful to be able to work with her more closely for my master's degree. I was able to learn so much through this research process and am extremely grateful to have been able to do it, even as it was a difficult challenge to overcome. I would also like to thank Dr. Michael Stoner for helping me with learning how to operate various machinery relevant to my research work and for always being willing and able to give me an extra hand whenever I needed it. I am also extremely thankful for the help of Cooper Banks with doing all my testing over my months of research; I could not have gotten so much work done without his willingness to work with me through those many hours of research. I would also like to thank Scott Black for his help with fabricating various parts necessary for my testing setup and for coming to the lab many times to give me assistance with setting up or modifying my testing device. I would also like to thank Arcosa lightweight for providing the expanded clay aggregate and General Shale for donating the masonry block and materials for the mortar.

Thanks to my family and friends for all their encouragement and love throughout all of my research work. I could not have made it through all of this without them and am so grateful!

TABLE OF CONTENTS

ABSTRACT.....	1
DEDICATION.....	2
ACKNOWLEDGEMENT.....	3
LIST OF FIGURES.....	6
LIST OF TABLES.....	8
LIST OF EQUATIONS.....	9
CHAPTER 1: INTRODUCTION.....	10
CHAPTER 2: LITERATURE REVIEW.....	12
Lightweight Aggregates in Concrete.....	12
Lightweight Aggregates in Masonry.....	14
Flexural Bond Strength Testing per ASTM C1072-13.....	19
CHAPTER 3: DEVICE DESIGN AND CAPACITIES.....	22
Purpose of Test Device.....	22
Final Design of Device.....	23
Device Capacity Calculations.....	28
Issues Encountered and Modifications to Device.....	32
CHAPTER 4: MATERIALS AND SPECIMEN PREPARATION.....	34
Aggregate and Mortar Properties.....	34
Mix Design for Final Batches.....	35
Preparation of C1072 for Bond Wrench.....	36
CHAPTER 5: TEST PROCEDURE.....	41
C1072 Installation Process.....	41
Flexural Tensile Test Process.....	43
Instrumentation Setup.....	43
Hydraulic Loading Procedure.....	43
Density Measurements.....	45
CHAPTER 6: RESULTS.....	47
Summary of Bond Wrench Results.....	47
String Potentiometer Displacement Results.....	50
Comparison of Data to Normal-Weight Specimens.....	50

Comparison to Modulus of Rupture Testing.....	54
Conclusion.....	55
Data Collection for Density-Based Lambda Factors.....	56
CHAPTER 7: CONCLUSION	58
REFERENCES	60
APPENDIX I: SPECIMEN PREPARATION	62
APPENDIX II: TESTING PROCEDURE.....	66
Setup.....	66
Safety Protocol	66
Test Procedure.....	67
Initial Contact	67
Load to Failure.....	67
Final Data Saving	67
APPENDIX III: CAPACITY CALCULATIONS	68
Initial Check on Upper Bound Expected Actuator Force Compared to Actuator Capacity	69
Check on Threaded Rod and Nuts to Attach the Specimen to the Plate	70
Check on Bolts from Member 6 to Plate on Masonry Specimen.....	72
Check on Epoxy Anchor Capacity (Masonry Breakout)	78
Check on Connections of Upper Actuator to Member 4.....	81
Summary	82
APPENDIX IV: STRING POTENTIOMETER DISPLACEMENT GRAPHS.....	83

LIST OF FIGURES

Figure 1. Parallel to Bed Joints (left) vs. Normal to Bed Joints (right)	16
Figure 2. ASTM C1072-13 Bond Wrench Testing Apparatus	21
Figure 3. ASTM C1072-13 Bond Wrench Frame and Elevation	21
Figure 4 Custom Moment Couple Schematic.....	23
Figure 5. Upper bolt connections to Member 6 using angles and 1-inch length bolts	24
Figure 6. Lower bolt connection to Member 3 using steel tubes.....	24
Figure 7. Member 6 being put into place using crane and angles.....	25
Figure 8. Angle connections between C1072 specimen and Member 6.....	26
Figure 9. C1072 Specimen installed in Bond Wrench and attached to Member 6.....	28
Figure 11. Actuator with Steel Spacers.....	32
Figure 12. Holes drilled in masonry	38
Figure 13. Threaded rod in drilled hole	38
Figure 14. Steel plate overlaying inserted threaded rod	39
Figure 15. Finished C1072 specimens with threaded rod.....	39
Figure 16. C1072 specimen with plates attached.....	40
Figure 17. Custom Bond Wrench Schematic.....	41
Figure 18. C1072 Specimen in Place.....	42
Figure 19. Upper Portion of Bond Wrench Attached	42
Figure 20. Coring Drill Setup	45
Figure 21. Lightweight vs. Normal-Weight Aggregate Bond Strength.....	53
Figure 22. Steel Plates Clamped to C1072 Specimen.....	62
Figure 23. Drilled Hole in C1072	63
Figure 24. Drilled Holes being Vacuumed	63
Figure 25. Threaded Rod in Drilled Hole	64
Figure 26. Threaded Rod Lined Up with Steel Plates	65
Figure 27. Steel Plates Being Aligned to C1072 Corners.....	65
Figure 28. Diagram showing profile of Bond Wrench device.....	68
Figure 29. Load path for moment application to masonry.....	68
Figure 30. C1072 specimen in Bond Wrench attached to Member 3	70
Figure 31. C1072 specimen installed in Bond Wrench and connected to Member 6.....	70

Figure 32. Member 6 being put into place on the upper half of C1072.....	72
Figure 33. Angle connections between C1072 and Member 6.....	72
Figure 34. Steel tube for connection between C1072 and Member 3.....	77
Figure 35. Actuator dimension diagram	81
Figure 36. Actuator 1 setup.....	81
Figure 37. 6/29/2022 Test String Potentiometers	83
Figure 38. 7/15/2022 Test String Potentiometers	83
Figure 39. 8/3/2022 Test String Potentiometers	84
Figure 40. 8/4/2022 Test String Potentiometers	84
Figure 41. 8/5/2022 Test String Potentiometers	85

LIST OF TABLES

Table 1. TMS 402-602 Predicted Bond Strengths for Various Mortar Types.....	17
Table 2. Custom Moment Couple Device and C1072 Specimen Properties	27
Table 3. ASTM C1072-13 Bond Wrench Device Weights and Specimen Properties.....	27
Table 4. Ratio of Tensile Strength to Square Root of Compressive Strength for Modulus of Rupture Testing.....	29
Table 5. Aggregate Properties.....	34
Table 6. Mix Design for Grout Batches.....	35
Table 7. Compression Test Results.....	35
Table 8. Tested Sample Strengths.....	47
Table 9. Predicted Strength.....	48
Table 10. Comparison between Bond Strength and Compression Stress.....	48
Table 11. Comparison to ASTM C1072-13 Bond Wrench Compression Stress.....	49
Table 12. TMS 402-602 Predicted Bond Strengths for Various Mortar Types.....	49
Table 13. Total Displacement of String Pots for Each Test	50
Table 14. Normal-Weight Grout Test Results	52
Table 15. Lightweight Concrete and Grout Results (Shrestha et al. 2022)	54
Table 16. Summarized Conclusions	55
Table 17. Grout Density Measurements	56
Table 18. Dried Mass Measurements.....	57

LIST OF EQUATIONS

Equation 1. Flexural Tensile Strength for Prisms Built of Solid Masonry Units	20
Equation 2. Flexural Tensile Strength for Prisms Built of Hollow Masonry Units.....	20
Equations 3. Calculations for Theoretical Moment Used for Capacity Checks	30
Equations 4. Calculations for anchor pull out capacity	31
Equation 5. Bond Strength Calculation	44
Equation 6. Compression Stress Calculation	44
Equation 7. Equilibrium Density Formula.....	46

CHAPTER 1: INTRODUCTION

Lightweight concrete is a material that has been studied by many researchers and has displayed benefits such as higher thermal conductivity (Cavalline, 2017), lower density/seismic mass, and internal curing (Bentz, Weiss, 2011). While lightweight concrete is approved and used in many circumstances, lightweight grout is not currently permitted in reinforced masonry design per the TMS 402/602-22 code. Allowing for lightweight grout construction by formulating a reduction factor for properties like tensile strength, shear strength, bond to reinforcement, and flexural bond strength in the TMS 402/602 code would greatly expand the viability of lightweight aggregates and further the possible applications in fully grouted masonry construction. This study contributes to building up the database of test results needed to inform such a reduction factor. Specifically, this research focused on measuring the flexural tensile strength of fully grouted masonry blocks using a moment couple device, modified from the standard bond wrench device that is described by ASTM C1072-13. This device required modification as the standard bond wrench device is only suitable for smaller masonry specimens and would not allow for the testing of the larger fully grouted specimens examined for this study. The moment couple device created for this study was designed by Clemson graduate student Stephen Wright to induce the same flexural tensile failure pattern on the larger C1072 specimens.

These measured strengths were then compared with the strengths of normal-weight grout to determine whether reduction factors would be necessary to account for strength differences between lightweight and normal-weight grout and allow for lightweight grout to be used more widely in masonry construction. This study focuses on one type of lightweight aggregate, expanded clay, which is used in two grout mixes; the density of these mixes was determined, as

well as per ASTM, to provide a second point of comparison to normal-weight grout and for use in future research applications.

This paper is organized into seven chapters. Chapter 1 introduces the paper and explains the scope and goals of this research study. Chapter 2 covers previous literature exploring the benefits and design considerations for lightweight concrete, as well as going over the current research on lightweight grout. The ASTM test for flexural tensile strength (ASTM C1072) is also explored in order to show why it was not viable for this study and to compare this device to the moment couple device created in this research. Chapter 3 looks at the overall design of the moment couple device, including changes that had to be made over the course of testing due to arising issues related to concerns with the bending capacity of the bolts used for connections between the masonry specimen and the outer moment couple device, as well as covering the calculations made as to the capacity of each component of the device, ensuring that none of the flexural strength tests would exceed these allowable strengths. Chapter 4 goes over the materials used for the creation of the ASTM C1072 masonry specimens and their grout mixes, as well as detailing the procedure for preparing these specimens for testing in the bond wrench device. Chapter 5 covers the specific details of the flexural tensile strength test itself, including how to load the C1072 specimens into the device and what steps to perform during the test. Chapter 6 goes through the results of these flexural strength tests and compares them to similar results from normal-weight grout. A determination is then made as to the necessity of reduction factors for the use of lightweight grout in construction. Finally, Chapter 7 concludes the paper and summarizes the contents of the study and its results.

CHAPTER 2: LITERATURE REVIEW

Lightweight Aggregates in Concrete

Lightweight aggregate has been used in a variety of contexts in concrete construction for many years due to its abilities to reduce the overall weight of structures and improve insulation. For example, Alaa Rashad's (2018) paper "Lightweight Expanded Clay Aggregate as a Building Material" found that incorporating lightweight aggregate into a concrete mixture could serve to make it more workable, and that the overall density of the hardened concrete mix can be reduced by between 35% to 44.4% depending on whether the lightweight aggregate is incorporated solely as a fine aggregate or as both fine and coarse aggregates. This study also found that the incorporation of some lightweight aggregates, such as the LECA aggregate studied here, could reduce the strength of concrete from 12.5% to 55.97% depending on the extent to which it was incorporated in place of normal-weight aggregate. While it was found that incorporating lightweight aggregate decreased its resistance to freeze/thaw and increased water absorption, it also increased overall thermal insulation, sound insulation, and fire resistance. Tara Cavalline's (2017) paper "Impact of Lightweight Aggregate on Concrete Thermal Properties" further supports Rashad's conclusions of the thermal conductivity benefits of lightweight aggregates in concrete, finding that the average thermal conductivities of two types of lightweight aggregates (SLWC and ALWC) are reduced by 23% and 60% respectively, as compared to normal-weight concrete. In *Influence of Internal Curing on Properties and Performance of Cement-Based Repair Materials*, by Dale Bentz, Scott Jones, Max Peltz, and Paul Stutzman (2015), it is found that the inclusion of lightweight aggregate provides a significant reduction in measured deformation of cement repair materials. It was also found that of the three internal curing agents examined for this research study, lightweight aggregate showed the highest compressive strength and modulus of rupture

while producing an equivalent or reduced drying shrinkage compared to repair materials without internal curing additions. In the paper “The effect of high temperature on compressive strength and splitting tensile strength of structural lightweight concrete containing fly ash” (2008), by Harun Tanyildizi and Ahmet Coskun, the authors explore the effect of high temperature on structural lightweight concrete containing fly ash. This study found that the compressive strength and splitting tensile strength of unfired lightweight concrete drops sharply after 800 degrees C. However, until this temperature point, lightweight concrete displays high resistance to temperature changes, which is enhanced by the inclusion of fly ash.

In the article “Direct Tensile Strength of Lightweight Concrete with Different Specimen Depths and Aggregate Sizes” by Se-Jin Choi et al. (2014), it was found that the inclusion of lightweight aggregate in concrete mixes corresponded to an overall reduction in strength, though this change was also due to different aggregate sizes as covered in this study. In “Size effect on tensile strength of lightweight aggregate concrete: A numerical investigation” (2022) by Yang Liu et al., it was found that lightweight aggregate decreases the strength of concrete mixes but that it can also mitigate the size effect of different aggregate sizes in these mixes. However, it was also found that concrete with higher strength caused by a lower water/cement ratio or a higher-strength lightweight aggregate showed a stronger aggregate size effect when under tension. The highest reduction ratio found in this study for the inclusion of lightweight aggregate was 0.58 for a W/B ratio of 0.22.

Lightweight Aggregates in Masonry

While lightweight grout is less commonly used than lightweight concrete due to the lack of acceptable standards pertaining to it, the design of lightweight masonry grout has been explored in some detail in various studies. For example, in “Material and structural properties of lightweight masonry grout” by Dillon K. Bane (2016), he displays that the strength of lightweight grout is dependent on the aggregate used, and that some mixes can be stronger than normal weight grout depending on the aggregate properties. In Hannah Polanco’s (2017) paper “Structural Lightweight Grout Mixture Design,” she discusses the procedure for creating a grout mix using lightweight aggregate, and the different properties gained based on changes in this procedure. For example, it is shown that soaking the aggregate before the mixing process significantly affects the compressive strength, but that this benefit decreases as the quantity of aggregate increases. She also found that grout made with lightweight aggregate more than reaches the required minimum strength of 2000 psi. In Daniel Rikli’s (2020) paper, “Comparing Strength and Modulus of Elasticity Values for Prisms Constructed with Lightweight and Normal Weight Grout,” he shows that at low compressive strengths, there is no statistical difference between normal-weight and lightweight grout prisms, but that at higher compressive strengths, lightweight grout cannot sustain the same loads and stresses and normal-weight grout. He suggests that a density modification factor could allow for the use of lightweight grout in masonry structures subject to these higher loads. Tara Cavalline’s (2017) paper “Impact of Lightweight Aggregate on Concrete Thermal Properties” also details the thermal conductivity benefits of lightweight grout, showing that grout mixtures including lightweight aggregates provide a 60% reduction in thermal conductivity as compared to normal-weight grout.

Research on masonry testing for different types of results was explored as a template for the test setups explored in this paper. One of these was “Behavior of Anchor Bolts in Concrete Masonry with Lightweight Grout” (2022) by Rumi Shrestha, Hannah Kessler, Laura Redmond, and Prasad Rangaraju. These tests showed that for axial tensile strength tests, these specimens displayed a higher tensile capacity than expected, meaning that an anchor bolt reduction factor was likely unneeded for lightweight grout construction. However, for the shear strength tests, the tested capacity resulted in ratios between tensile and compressive strength lower than 1.0, meaning that a reduction factor would be necessary for these applications. In “Diagonal Tensile Strength and Lap Splice Behavior of Concrete Masonry Assemblies with Lightweight Grout” (2022) by Rumi Shrestha, Laura Redmond, and Jason Thompson, diagonal tensile strength tests and lap splice tests were performed on masonry specimens using lightweight to compare their performance to that of samples using normal-weight grout. Overall, this study found that a reduction factor for the use of lightweight grout for diagonal tensile strength and lap splice strength was merited, similar to the reduction factors used for lightweight grout in concrete.

Flexural Bond Strength of Grouted Masonry

Literature covering the more general characteristics and flexural behavior of masonry structures was covered as well. In the paper “Behavior Characteristics of Concrete Masonry” by Ahmad Hamid (1979), in which he displays that for hollow masonry blocks, the average flexural tensile strengths normal to the bed joints are often very low and close to allowable stress values, while the flexural tensile strengths parallel to bed joints are usually several times higher. The difference between loading parallel to bed joints and loading normal to bed joints is shown below in Figure 1. However, it is shown that adding grout to these hollow masonry blocks greatly increases their flexural tensile strength normal to the bed joints, to a higher degree than that of solid masonry blocks. It is also shown that the percentage of filling in the masonry cells significantly affects their flexural tensile strength.

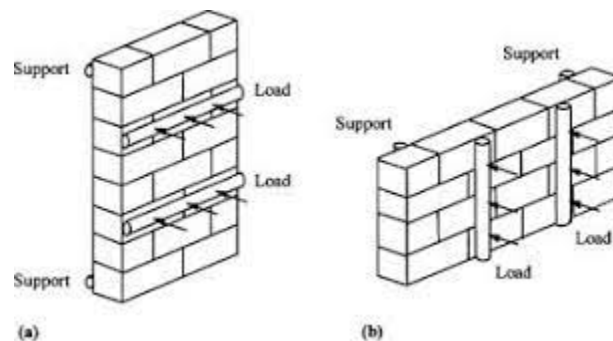


Figure 1. Parallel to Bed Joints (left) vs. Normal to Bed Joints (right)

In “Flexural Tensile Strength of Partially Grouted Concrete Masonry” (1988), by Ahmad Hamid, Sammu Chandrakeerthy, and Omar Elnawawy, they explore the strength benefits of different levels of grouting masonry specimens, showing that moving from grouting every fourth core in a masonry wall to grouting every core increases the flexural tensile strength of the structure from between 72% to 397%. It was also found that the factor of safety for fully grouted concrete

masonry from the equation in ACI-530/ASCE-5 is higher than that of partially grouted masonry, but that this factor of safety can vary considerably based on the extent of grouting used. The current predictions for flexural tensile strength based on different mortar types from TMS 402-602 are shown below in Table 1, showing a similarly wide range in predicted strength based on the extent of grouting and the subsequent direction of loading, consistent with the findings in the study discussed here.

Table 1. TMS 402-602 Predicted Bond Strengths for Various Mortar Types

Direction of flexural tensile stress and masonry type	Mortar types			
	Portland cement/lime or mortar cement		Masonry cement or air entrained portland cement/lime	
	M or S	N	M or S	N
Normal to bed joints				
Solid units	133 (919)	100 (690)	80 (552)	51 (349)
Hollow units ²				
UngROUTED	84 (579)	64(441)	51 (349)	31 (211)
Fully grouted	163 (1124)	158 (1089)	153 (1055)	145 (1000)
Parallel to bed joints in running bond				
Solid units	267 (1839)	200 (1379)	160 (1103)	100 (689)
Hollow units				
UngROUTED and partially grouted	167 (1149)	127 (873)	100 (689)	64 (441)
Fully grouted	267 (1839)	200 (1379)	160 (1103)	100 (689)
Parallel to bed joints in masonry not laid in running bond				
Continuous grout section parallel to bed joints	335 (2310)	335 (2310)	335 (2310)	335 (2310)
Other	0 (0)	0 (0)	0 (0)	0 (0)

¹ The values in this table shall not be applicable to structural clay tile unit masonry (ASTM C34, ASTM C56, ASTM C126, ASTM C212)

² For partially grouted masonry, modulus of rupture values shall be determined on the basis of linear interpolation between fully grouted hollow units and ungrouted hollow units based on amount (percentage) of grouting.

In “Flexural Bond Strength of Unreinforced Grouted Masonry Using PCL and MC Mortars” (1999) by Russell Brown and John Melander, the materials used in grout mixtures are studied as to how they affect the ultimate flexural tensile stress of unreinforced masonry specimens. Specifically, the researchers examined the difference in ultimate flexural tensile stress between specimens using masonry mortar cement and specimens using portland cement/lime mortars. The 1999 masonry building code recommended a 40% reduction factor for Type M and

S mortar and a 50% reduction for Type N mortar. To find whether these reduction factors were suitable, masonry walls were studied for their flexural strength with applied load normal to the bed joints. The data from these tests showed that much greater factors of safety were necessary for masonry specimens using masonry mortar cement as opposed to specimens using portland cement mortar. This data also showed that factors of safety were higher for grouted masonry units than hollow units.

In the research study “Flexural Tensile Strength of Partially Grouted Concrete Masonry” (1992), researchers Ahmad Hamid, et al, tested various partially grouted masonry assemblies to find their flexural tensile strength. For these tests, the standard ASTM C1072 bond wrench device was used, as described in the below section. Model masonry wall assemblies were constructed using partially grouted specimens on which a load normal to the bed joints was induced. These specimens were smaller in dimension in order to adhere to the specifications for the bond wrench. The results of this study indicated that for more regular grouting, the flexural tensile strength of the masonry assemblies improved drastically, and that the overall flexural tensile strength was significantly variable based on the amount of grouting used in the masonry assemblies.

Flexural Bond Strength Testing per ASTM C1072-13

The standard flexural bond strength test is detailed in ASTM C1072-13, covering the performance of this test using a standard bond wrench device. This test is applicable for stacked clay or concrete masonry units bonded with mortar, which have an applied force normal to the bed joint from the bond wrench device. The breaking strength of these masonry units at the mortar joint gives an indication of the flexural tensile strength of the mortar/unit bond used to connect the concrete masonry units. The standard design of the bond wrench device applicable to this test is shown below in Figure 2. While this test is useful for finding the flexural tensile strength of masonry walls connected with mortar under loads normal to their bed joints, it is not applicable for fully grouted masonry units as tested in this study. This is due to the dimensions of this standard bond wrench device, which only allows for masonry units 3.625" wide by 2.25" high with a length between 7" and 7.625". The fully grouted masonry units used for this lightweight grout study have dimensions 7.625" wide by 7.625" high with a length of 15.625", and therefore would not fit within this standard bond wrench testing apparatus. This apparatus also only applies its load in a single direction to break the masonry at the mortar joint, and uses clamping bolts to hold the masonry, which is appropriate for the lower overall strength of mortar but would not be sufficient for the higher strength of the fully grouted concrete masonry units used in this study. A more detailed schematic of the standard bond wrench testing device is shown in Figure 3, making the dimensions clearer and displaying its ineffectiveness for the test at hand. While this test is useful in that it allows for more than two stacked masonry units to be loaded at a time, increasing the speed of overall testing, its dimensions and capacity limitations make it an unsuitable method for fully grouted masonry units. The ASTM C1072 equations for flexural tensile strength are shown below in Equation 1 and Equation 2, where the former is the equation for specimens built of solid masonry units and the latter is for specimens built of hollow masonry units. Equation 1 for solid masonry

units is based on the applied moment load from the loading arm as well as the weight of the loading arm, in conjunction with the area of the masonry unit defined by the width b and the depth d . L represents the distances from the center of the prisms in the bond wrench device to the loading point from the moment arm. In Equation 2, the equation is modified to include the section modulus S rather than the area in b and d in order to account for the hollow nature of the masonry prism.

$$F_g = \frac{6(PL + P_l L_l)}{bd^2} - \frac{(P + P_l)}{bd} \quad (\text{A3.1})$$

where:

- F_g = gross area flexural tensile strength, psi (MPa),
- P = maximum applied load, lbf (N),
- P_l = weight of loading arm, lbf (N), (see [Appendix X2](#)),
- L = distance from center of prism to loading point, in. (mm),
- L_l = distance from center of prism to centroid of loading arm, in. (mm) (see [Appendix X2](#)),

Equation 1. Flexural Tensile Strength for Prisms Built of Solid Masonry Units

$$F_n = \frac{PL + P_l L_l}{S} - \frac{P + P_l}{A_n} \quad (\text{A3.2})$$

where:

- F_n = net area flexural tensile strength, psi (MPa),
- S = section modulus of the net bedded area of the prism, in.³ (mm³), and
- A_n = net bedded area of the prism, in.² (mm²).

Equation 2. Flexural Tensile Strength for Prisms Built of Hollow Masonry Units

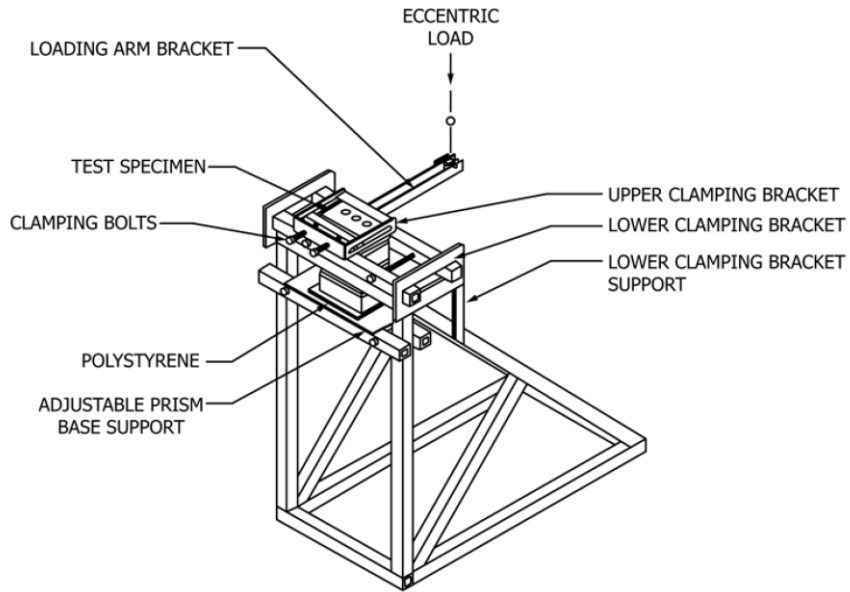


Figure 2. ASTM C1072-13 Bond Wrench Testing Apparatus

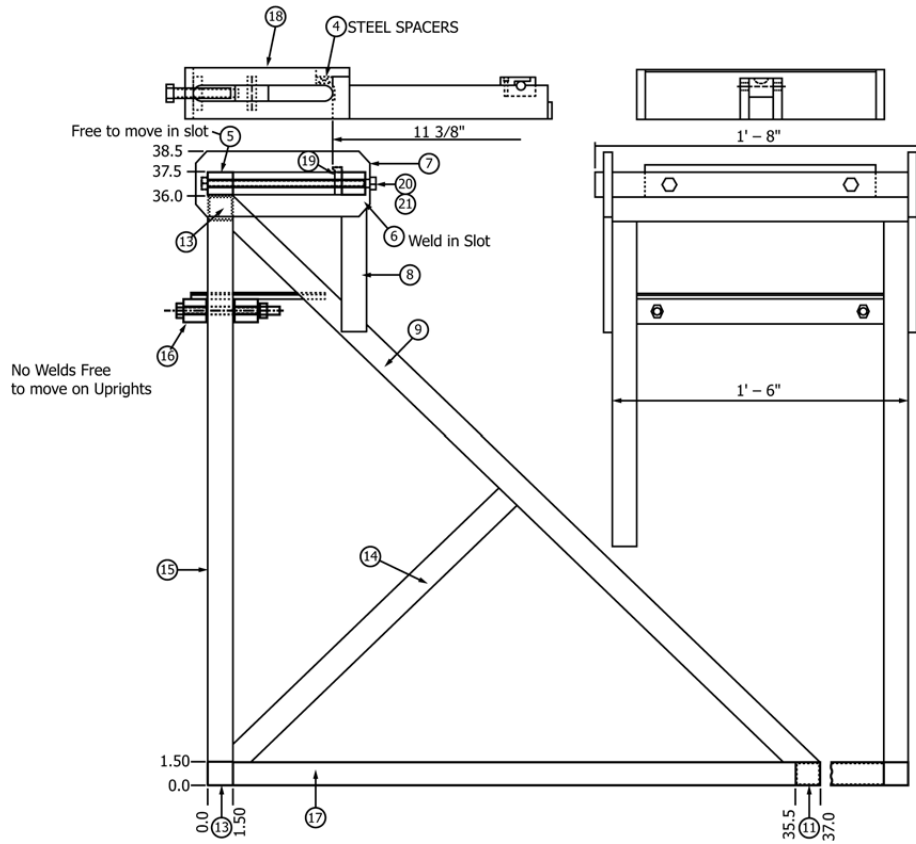


Figure 3. ASTM C1072-13 Bond Wrench Frame and Elevation

CHAPTER 3: DEVICE DESIGN AND CAPACITIES

Purpose of Test Device

The moment couple test device was designed to induce a flexural failure mode across the mortar joint of fully grouted C1072 masonry specimens. This would be done by inducing a moment on the upper half of the specimen from two actuators, as is shown in Figure 4 below, where the bond wrench device is attached to the floor at two points from Member 3. This failure mode is representative of out-of-plane flexure that could be induced in masonry blocks in a structure due to wind pressure.

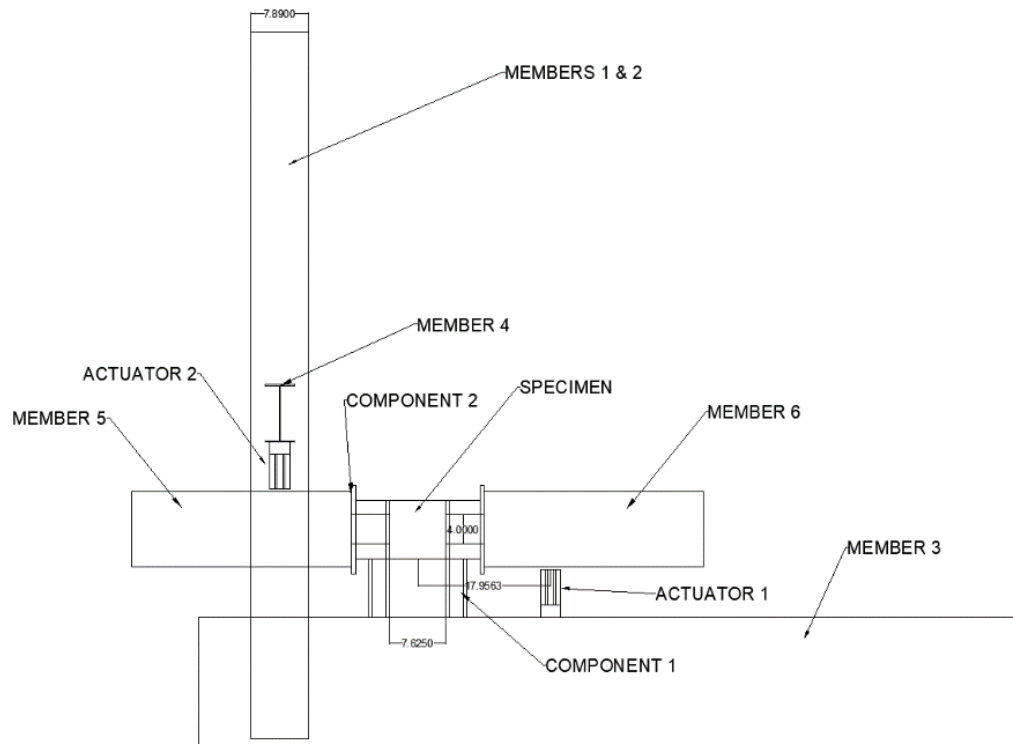




Figure 4.

Overall Schematic of Moment Couple Device (top)

Moment Couple Device Set-Up (bottom)

Final Design of Device

The load path for the applied moment begins at each actuator and travels through Member 5/6 to the angle connection between component 2 and the steel plates attached to the upper half of the C1072 specimen. These angles transfer a bending force by relying on the shear strength of the 1-inch length bolts connecting them together. This force creates a moment couple at the bolt connections attaching to the steel plates, as is shown in Figure 5 below. The calculations for the induced moment load from the moment arms based on the output from Actuator 1 are shown in Equation 1 at the end of this chapter. The connection at the base from component 1 to the masonry is similar, but the loads are transferred directly through bolts with shear sleeves (Figure 6).



Figure 5. Upper bolt connections to Member 6 using angles and 1-inch length bolts



Figure 6. Lower bolt connection to Member 3 using steel tubes

Note that for the final design of the device, the internal components for connections from the outer device to the C1072 specimen were re-designed. One of these was re-designed by using match-drilled angles (shown in Figure 5) to replace the longer bolts for the upper connection, with 1-inch length bolts connecting the angles together. This was to account for the insufficient bending capacity of the Grade 8 bolts when transferring force over the longer distance of the upper bolt connection. By using angles instead, this bending force was transferred to shear force through the shorter Grade 8 bolts, for which they were sufficient. For the lower bolt connection, 1-inch-long steel sleeves were placed over the Grade 8 bolts and fastened down to the outside of the plates using nuts. These lower bolts are also used to center and secure in place the C1072 specimen by using nuts to fasten the bolts to the outer and inner walls of the bond wrench box, shown as Component 2 in Figure 4.



Figure 7. Member 6 being put into place using crane and angles

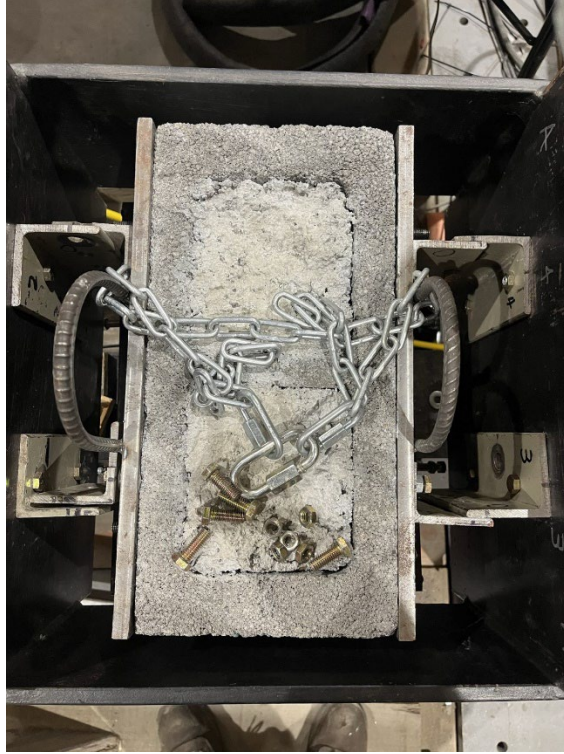


Figure 8. Angle connections between C1072 specimen and Member 6

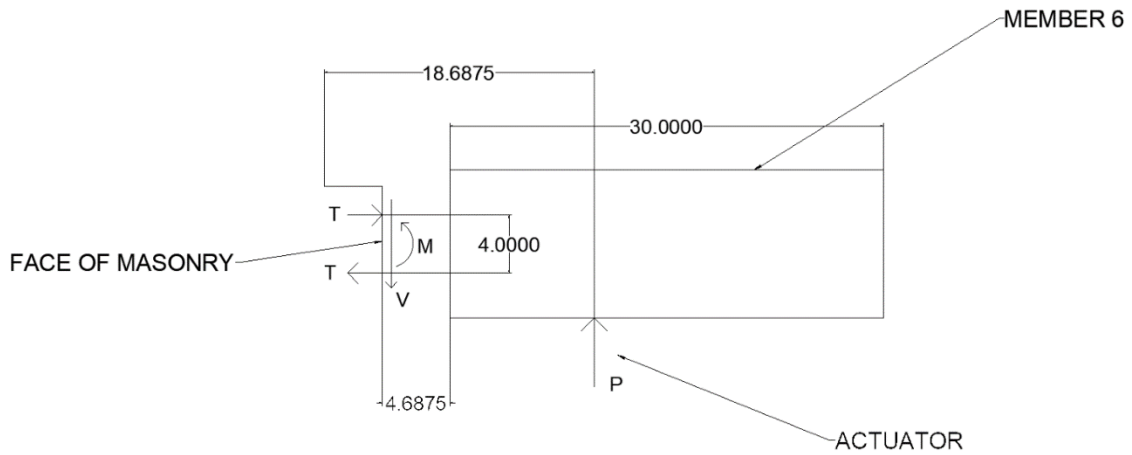


Figure 9. Load path from Actuator 1

The calculated weights for the custom moment couple test components are shown below in Table 2. The dimensions of the upper portion of the masonry specimen are detailed and calculated as the self-weight of 52.6 lb. This weight is accumulated with the weights of the arms,

plates, and box plates that make up the upper portion of the moment couple device and contribute to the compression force experienced during testing, as well as the bolts and face plates for the C1072 specimens. The weights of these parts of the device come out to a total of 243.8 lb. Shown in Table 3 are similar values for the ASTM bond wrench device, covered in Chapter 2. This device has an upper clamp which attaches to the smaller masonry specimens, and therefore the overall compression force applied to the device during testing is much lower, as can be seen by the specimen self-weight of 4.3 lb and the upper clamp weight of 39.8 lb. These weights are based on a standard masonry density of 120 lb/ft³. However, when you compare the compressive stress induced in each device, they are very similar with the ASTM C1072 device, inducing 1.6 psi of compression stress on a standard modular clay brick and the moment couple device inducing 2.5 psi of compression on fully grouted concrete blocks.

Table 2. Custom Moment Couple Device and C1072 Specimen Properties

SW (lb)	b (in)	h (in)	A (in ²)	I (in ³)	Arms W (lb)	8" x 17.375" Plates W (lb)	12"x18" Plates W (lb)	Misc. Parts W (lb)
52.6	15.625	7.625	119.14	577.24	95.0	39.5	61.3	48

Table 3. ASTM C1072-13 Bond Wrench Device Weights and Specimen Properties

h (in)	b (in)	L (in)	A (in ²)	SW (lb)	Upper Clamp Weight (lb)
2.25	3.625	7.625	27.64	4.32	39.84

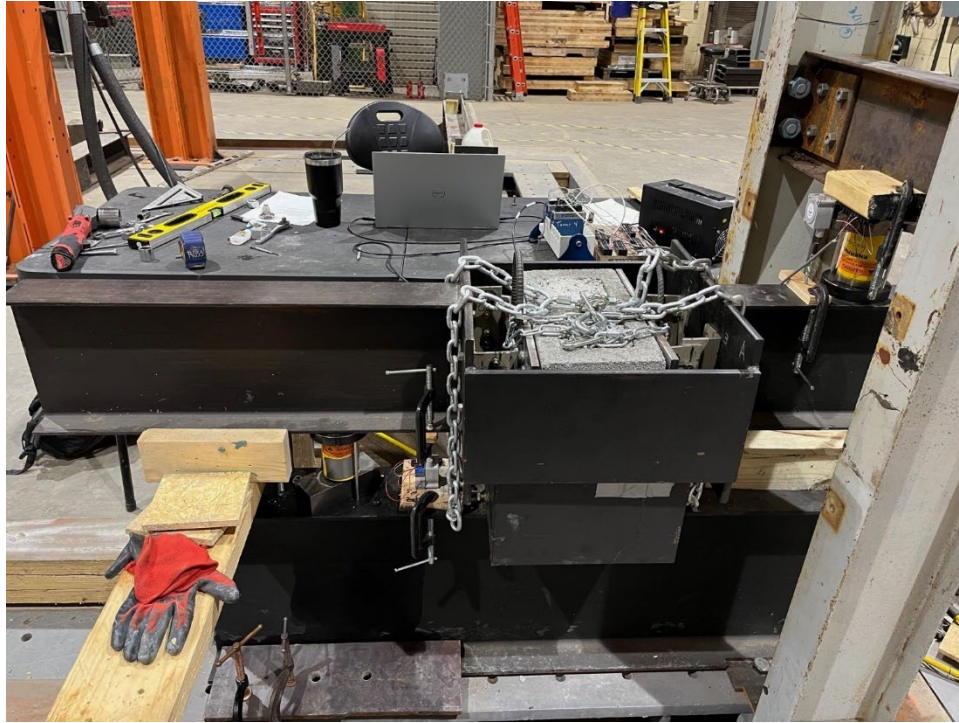


Figure 9. C1072 Specimen installed in Bond Wrench and attached to Member 6

Device Capacity Calculations

Each component of the device was checked for its maximum capacity to ensure that they would be able to withstand any applied loads during testing of the C1072 specimens, based on an assumed maximum actuator output of 4.213 kips during testing. The assumed 4.213-kip output came from assuming the specimens would have at most a 3000-psi grout strength and an $\frac{f_r}{\sqrt{f_g}}$ ratio of 0.6 based on testing of grout beams by Shrestha (2022) as shown in Table 4. This table shows overall averages for each material type, accounting for some outliers. However, when taken as a whole, the data for expanded clay grout is conservative for the assumption of 0.6.

Table 4. Ratio of Tensile Strength to Square Root of Compressive Strength for Modulus of Rupture Testing

Material Type	Bond Strength Average	Compression Strength Average	Ratio	$f_r/\sqrt{f_g}$
	f_r (ksi)	f_g (ksi)	f_r/f_g (%)	
Lightweight Concrete	0.5886	5.3892	10.9	0.25
Lightweight Grout	0.5794	4.2451	13.6	0.28
Expanded Clay Grout	0.6166	3.3745	18.3	0.34
Expanded Slate Grout	0.8101	5.1226	15.8	0.36

The checks conducted included the shear and tension strength of the threaded rod embedded in the specimens while under loading, the shear and tension strength of the connecting bolts between the bond wrench device and the C1072 specimens, the flexural strength of the angles for the upper bond wrench attachment, the capacity of the actuator attachment wiring for the lower actuator, the bending strength of the steel plates attached to the C1072 specimen, and finally the pull-out strength of the epoxy used to embed the threaded rods in the C1072 specimens. A full set of calculations can be found in Appendix III. Of these components, the critical loading point was found to be the epoxy pull-out strength. The factored tension capacity for the epoxy for each embedded rod was found to be 4.088 kips. Based on a compressive strength of 3500 psi for the grout, a force of 4.077 kips would be induced on each epoxy connection, nearly reaching their capacity. For this reason, it was determined that this epoxy connection was the limiting factor and that a grout mix with a compressive strength higher than 3500 psi could not be tested in this device.

“INPUTS”	
“Compressive Strength”	$f_g := 3000 \text{ psi}$
“Compression Area”	$A := 15.625 \cdot \text{in} \cdot 7.625 \cdot \text{in} = 119.141 \text{ in}^2$
“Member Self-Weight”	$P_{SW} := \frac{19 \cdot \text{lb} \cdot \text{ft}}{\text{ft}} \cdot 30 \cdot \text{in} = 0.048 \text{ kip}$
“Modulus of Rupture”	$f_r := 0.6 \cdot \sqrt{\frac{f_g}{1000}} \cdot \text{ksi} = 1.039 \text{ ksi}$
<i>“Taken from Figure 8b in Tensile and Shear Behavior of Anchor Bolts”</i>	
“Full Moment Arm Length”	$L := 2 \cdot 18.6875 \cdot \text{in}$
“Compression Block Depth”	$c := 3.8125 \cdot \text{in}$
“Moment of Inertia”	$I := \frac{(15.625 \cdot \text{in}) (7.625 \cdot \text{in})^3}{12} = 577.243 \text{ in}^4$
“Member Length”	$L_{mem} := 30 \cdot \text{in}$
“Screw Gap Length”	$L_{gap} := 4.6875 \cdot \text{in}$
“OUTPUTS”	
“Maximum Stress”	$\sigma := f_r = 1.039 \text{ ksi}$
“Moment”	$M := \frac{I}{c} \cdot \left(\sigma + \frac{2 \cdot P_{SW}}{A} \right) = 157.468 \text{ kip} \cdot \text{in}$
“Individual Actuator Output”	$P := \frac{M}{L} = 4.213 \text{ kip}$
“Maximum Actuator Output for RCH121”	$P_{max} := 27.6 \cdot \text{kip}$

Equations 3. Calculations for Theoretical Moment Used for Capacity Checks

“Anchor Pull-Out Check (Epoxy Capacity)”

“Compressive Strength” $f_g := 3500 \text{ psi}$

“Compression Area” $A := 15.625 \cdot \text{in} \cdot 7.625 \cdot \text{in} = 119.141 \text{ in}^2$

“Member Self-Weight” $P_{SW} := \frac{19 \cdot \text{lb}_f}{\text{ft}} \cdot 30 \cdot \text{in} = 0.048 \text{ kip}$

“Modulus of Rupture” $f_r := 0.15 \cdot f_g \cdot \text{psi} = 0.525 \text{ ksi}$

Revised to 15% of f_g based on initial testing (to determine true system limit)

“Full Moment Arm Length” $L := 2 \cdot 18.6875 \cdot \text{in}$

“Compression Block Depth” $c := 3.8125 \cdot \text{in}$

“Moment of Inertia” $I := \frac{(15.625 \cdot \text{in}) (7.625 \cdot \text{in})^3}{12} = 577.243 \text{ in}^4$

“Member Length” $L_{mem} := 30 \cdot \text{in}$

“Screw Gap Length” $L_{gap} := 4.6875 \cdot \text{in}$

“Maximum Stress” $\sigma := f_r = 0.525 \text{ ksi}$

“Moment” $M := \frac{I}{c} \cdot \left(\sigma + \frac{2 \cdot P_{SW}}{A} \right) = 79.61 \text{ kip} \cdot \text{in}$

“Individual Actuator Output” $P := \frac{M}{L} = 2.13 \text{ kip}$

$M_{th} := P \cdot \left(\frac{L}{2} - c \right) + P_{SW} \cdot \left(\frac{L_{mem}}{2} + L_{gap} \right) = 32.619 \text{ kip} \cdot \text{in}$
“moment on one side of masonry”

$T := \frac{M_{th}}{S} = 8.155 \text{ kip}$ “Tension induced in each group of rods”

$T_{cap_unfactored} := 1.490 \text{ kip} \cdot 5 = 7.45 \text{ kip}$

Equations 4. Calculations for anchor pull out capacity

Issues Encountered and Modifications to Device

While attempting to use bond wrench device for flexural strength tests, issues were encountered with the original design which had to be addressed. Initially a steel component shown in Figure 3 was designed in order to create a more uniform loading surface for the lower actuator but was ultimately removed as it didn't allow for adequate stroke to break the specimens during loading. To circumvent this, steel spacers were added underneath the actuator as shown in Figure 11 below. Spacers were also added to the loading beam under the upper actuator attached to Member 4 for the same purpose. For the connection between Member 6 and the upper section of the C1072 specimens, the device was initially designed to use long bolts that would attach directly to the steel plates.



Figure 11. Actuator with Steel Spacers

However, during capacity calculations, it was discovered that the bending capacity of Grade 8 bolts was not sufficient for the 8” bolt length that would be required for those connections. The angles shown in Figure 4 were added to strengthen the bending capacity of this connection. These angles are each connected by two 1-inch length bolts, thereby converting this bending force into shear force across a smaller distance. If these connections are joined tightly, this solution circumvents the bolt capacity issue experienced previously. This issue would also be a problem for the lower bolts, though not to as great of a degree, as the span length is reduced. For these bolts, a steel sleeve was added over the bolts in order to increase their stiffness and render the bolts less susceptible to bending while being loaded.

CHAPTER 4: MATERIALS AND SPECIMEN PREPARATION

Aggregate and Mortar Properties

Lightweight aggregates were used for the grout used in the ASTM C1072 and ASTM C1019 specimens. This came in the form of Arcosa aggregate consisting of expanded clay, in which the coarse aggregate had a lower relative density than the fine aggregate. Standard 8” CMU blocks were used for C1072 specimens using Type S Mortar Cement for mortar joint connection. This lightweight aggregate also conforms to ASTM C330 in terms of their gradation as shown below in Table 5. This aggregate is explored in more detail in a paper by Rumi Shrestha and Laura Redmond entitled “Diagonal Tensile Strength and Lap Splice Behavior of Concrete Masonry Assemblies with Lightweight Grout,” in which the Arcosa expanded clay aggregate is used in testing, as well as an alternate form of lightweight expanded slate aggregate which was not covered in this study.

Table 5. Aggregate Properties

Physical Property	Expanded clay coarse	Expanded clay fines
Relative density (OD)	0.92	0.88
Relative density (SSD)	1.17	1.35
Specific Gravity (SG)	1.17	1.35
Absorption (%)	27.49	52.68
Gradation		
Sieve Size	Cumulative % weight by passing	
½ in	100	100
3/8 in	100	100
#4	30.6	100
#8	2.1	69.8
#16	1.3	43.6
#50	0.8	13.9
#100	0.5	9.8
#200	0.2	-

Mix Design for Final Batches

For the final batches for testing, two grout mixes were created using the Arcosa lightweight aggregate. The mix designs for both final batches are shown in Table 6 below in terms of weight in pounds, as well as the slump for each batch. These mixes were targeting an overall grout volume of about 3.9 cubic feet, as the mixer used had a usable volume of 4 cubic feet. The targeted slump for these mixes was between eight and ten inches, which was achieved with each batch. The compression strength of each batch of grout was determined using ASTM C1019 grout prisms and the results indicated that the grouts complied with the 2,000-psi minimum compression strength of ASTM C476, but batch 1 did not achieve this strength by the 28-day mark. The results of these compression tests are shown below in Table 6, where the three values in the upper portion of each region denote the specific compression strength readings, while the lower value for each region denotes the average of those three readings. Note that a lower capacity grout was targeted for these initial tests to avoid getting too close to the moment couple test device capacity.

Table 6. Mix Design for Grout Batches


Final Mix Designs	Components (lb)				Slump (in)
	Coarse Agg	Fine Agg	Cement	Water	
Arcosa 1	67.2	174.4	110.0	12.5	8.5
Arcosa 2	61.0	158.3	99.8	13.4	8.3

Table 7. Compression Test Results

Batch	Compression Tests (psi)								
	7-Day			28-Day			Final		
Arcosa 1	1404	1350	1225	1587	1732	1698	1989	2040	2018
	1326			1672			2015		
Arcosa 2	1860	1802	1881	2067	2147	2056	2565	2638	2604
	1847			2090			2602		

Preparation of C1019 and C1072 Specimens for Moment Couple Test

To prepare the C1072 and C1019 specimens, a procedure is followed according to ASTM C127 and ASTM C138 for the specific sizes of the specimens and the amount of time for which they must be cured. The aggregate for the grout mix is weighed while dry and first soaked for 72 hours and then dried for 24 hours by laying it on elevated plastic sheeting covered by a tarp. This ensures that the aggregate stays damp while not being fully saturated. After this process, the necessary amount of cement powder and water is weighed out and the mixing process can begin. First, the coarse and fine aggregates are added and combined, and then cement powder and water are added in small batches, testing the mix for slump periodically until it reaches the desired consistency. After this the mix is placed in the forms for the C1019 and C1072 specimens. The ungrouted C1072 specimens consist of two hollow CMU blocks stacked with mortar in the center. This mortar mix consists of mortar cement, sand, and water. Grout mix is placed into the voids in the C1072 specimen, using a rod to tamp down the mixture about 20 times when the mixture reaches each third point of the void. For the C1019 specimens, CMU blocks are used to create a three-inch square void into which grout mix can be placed. This mixture is also tamped down as the void is filled, using a tamping rod about ten times when the space is half full. When the C1072 and C1019 specimens are filled with grout, they are covered with plastic sheeting. After 24 hours, the C1019 specimens are removed from their molds and relocated to a fog room to await compression testing. The C1072 masonry prisms remained covered with plastic sheeting for 28 days to cure before testing.

To prepare the C1072 specimens for testing in the bond wrench , twelve holes are first drilled on each side, with six holes equally spaced on each CMU block face, as shown in Figure 12. Pilot holes are first drilled through the metal plates that will be finally attached using a

3/8" masonry drill bit, in order to ensure that they are in the correct locations. Afterwards these metal plates are removed and the final 2.5" deep holes are drilled using a 1/2" masonry drill bit, the depth of which is shown in Figure 13. After these holes are drilled, a vacuum is used to remove any excess dust that resulted from the drilling process, and then the holes are filled with SET-XP epoxy. Threaded rod pieces of 4" length and 3/8" diameter are placed in each hole, displacing the epoxy. Any excess epoxy that is pushed out of the holes is cleaned away using paper towels. Afterwards, wooden spacers are placed on the face of the masonry and the final metal plates are placed over these with the threaded rod feeding through the holes in the metal plates. The plates are then aligned with the corners of the CMU blocks and clamped down to ensure they do not slide, as shown in Figure 14. The epoxy is allowed to set for 4-8 hours before the C1072 specimens are rotated and the process is repeated. Once this process is finished, the specimens should appear as shown in Figure 15 below. After the threaded rods are set in place on both sides, the metal plates are secured to the specimen by placing them over the threaded rods and using nuts to secure the plates in place, as shown in Figure 16 below.

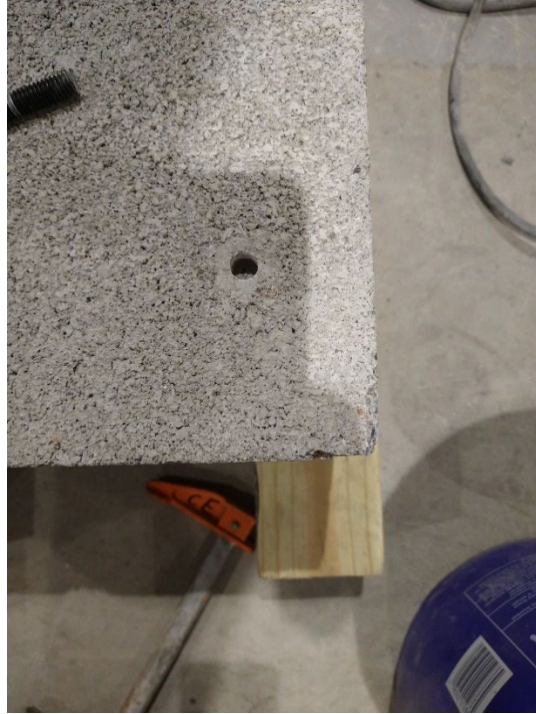


Figure 12. Holes drilled in masonry



Figure 13. Threaded rod in drilled hole



Figure 14. Steel plate overlaying inserted threaded rod



Figure 15. Finished C1072 specimens with threaded rod



Figure 16. C1072 specimen with plates attached

For these drilled holes mentioned above, there were concerns about cracking through the interface between the holes on each side. To ensure that this was not occurring during the tests, initial test specimens were cut in half after drilling was performed to check for any cracking patterns across the joint. No damage or cracking was seen between the drilled holes, and therefore it was assumed that this failure pattern would not be a concern during testing.

CHAPTER 5: TEST PROCEDURE

C1072 Installation Process

Once the C1072 specimens were fully prepared for testing, with plates attached, a rolling crane was attached to the steel hooks on the upper plates of the specimen, and it was moved into position in the bond wrench device, as is shown in Figure 17. The eight bolts for the lower portion of the bond wrench were screwed into the corresponding threaded holes in the lower plates of the C1072 specimen, while also being guided through 3/8" inner-diameter steel tubes. These tubes were secured to the lower plates using nuts, and the bolts were kept in a fixed position by tightening nuts down to the inner and outer walls of Components 2 shown in Figure 17 below.

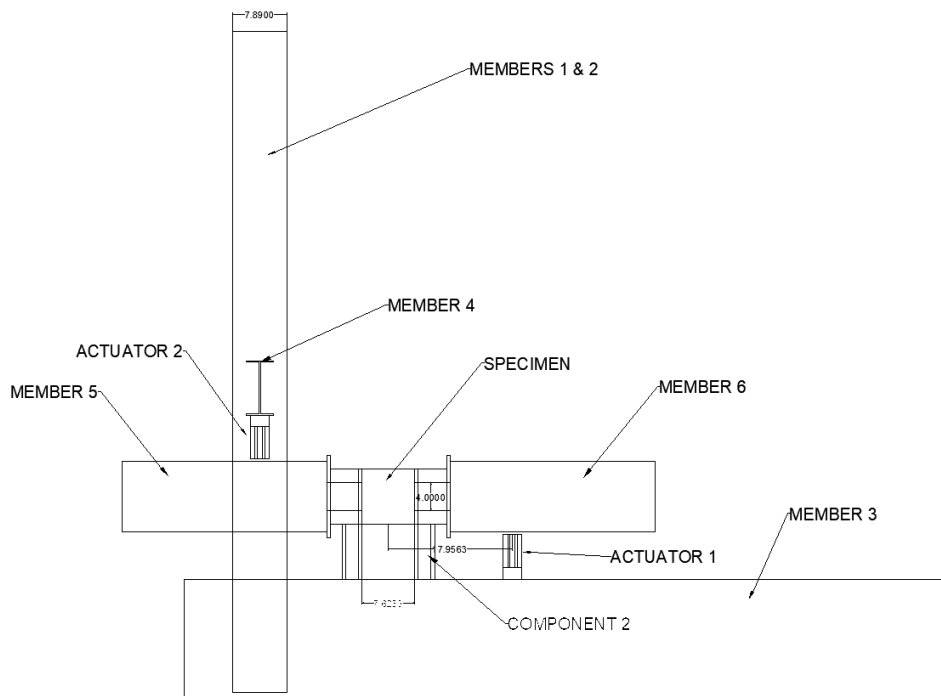


Figure 17. Custom Bond Wrench Schematic



Figure 18. C1072 Specimen in Place

Afterwards, Member 4 was unbolted from Members 1 & 2 and lifted to allow Member 6 to be put into place. Member 6 was lowered over the specimen by a crane, and, and the angle pieces were matched between Member 6 and the angles on the upper plates for the C1072 specimen, as shown in Figure 18. When these angles were bolted together, Member 4 was lowered back down into position and bolted into place.

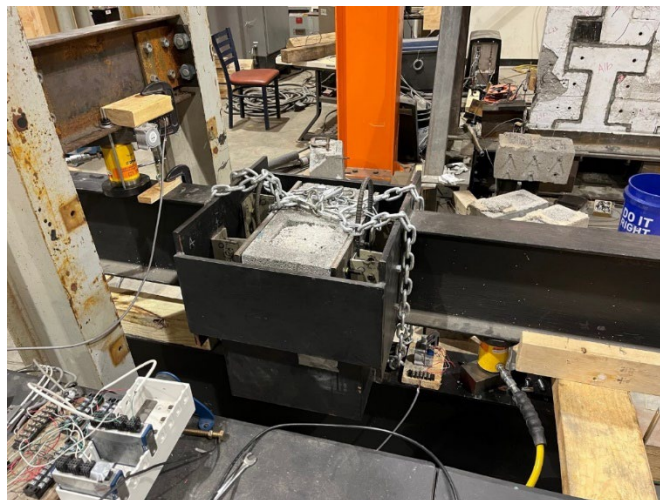


Figure 19. Upper Portion of Bond Wrench Attached

Flexural Tensile Test Process

Instrumentation Setup

Before the test can begin, all instruments need to be secured properly and tested to ensure that they will give an accurate reading during the test. The upper actuator attached to Member 4 and lower actuator attached to Member 3 are centered and tightened down to secure them in place. Hydraulic hoses are attached to upper and lower actuators and connections are tightened. The string pot attached to the upper actuator is secured to both Member 4 and Member 5 and is centered to ensure an even reading. The string pot for the lower actuator is attached to both Member 3 and Member 6 and centered, meaning that each string pot is 6” from the outside face of Component 2 and approximately 11” from the center of the C1072 specimen. Both string pots are tested to ensure they’re giving a correct output and the pressure gauges are tested to confirm that they are reading properly and that the cameras for recording them are oriented correctly. A data acquisition system is used to continuously record the string pot displacement and the pressure in each hydraulic, then convert this pressure to the force based on the internal loading area of the hydraulic. This factor was confirmed via pretesting in a universal testing machine.

Hydraulic Loading Procedure

After all string pots and pressure gauges are secured and tested, the hydraulic splitter is opened, and the hydraulic pump is operated until the upper actuator has contacted Member 5 and the lower actuator has contacted Member 6. At this point, the test can begin, and the recording is begun for the instrumentation on DAQ Scribe and for the cameras redundantly monitoring the pressure gauges. The hydraulic pump is operated at a consistent pace until the specimen has broken at the mortar joint, such that the total time for breaking the specimen is between one and three

minutes. The loading rate and test timing of one to three minutes is taken from ASTM E518, which details the impact of the loading rate during testing on the overall strength of the specimen. These specifications display that during a faster test time, a specimen will appear stronger, as the failure load is higher than would be required with more even loading. Therefore, by conforming to a loading rate of one to three minutes to reach ultimate breaking strength, the true bond strength of the specimen can be determined.

Once the specimen is broken, the pressure in the hydraulic pump is released so that the system is unloaded and safe to approach. The recordings for DAQ Scribe and the cameras are stopped, and the data is saved. The maximum force output from the test is then used to find the bond strength for each test. The flexural bond strength is calculated for each test by Equation 5:

$$(5) f_r = \frac{-SW}{A} + \frac{M \frac{h}{2}}{I}$$

where SW is the self-weight of the masonry, as calculated based on the grout and CMU density, and the weight of the device (242.6 lb., 1079.14 N), A is the cross-sectional area of the grouted CMU, M is the moment applied by the two actuators shown in Figure 7, $h/2$ is the distance to the maximum tensile stress location from the neutral axis (3-13/16 in, 9.684 cm), and I is the moment of inertia across the axis of bending, as calculated for a general sample based on standard CMU dimensions. The compression stress for each test is calculated by Equation 6:

$$(6) C_s = \frac{SW+W}{A}$$

Where SW is the self-weight of the masonry, W is the self-weight of the free portions of the bond wrench device, and A is the cross-sectional area of the masonry unit. These values differ between the custom bond wrench device used in this test and the standard ASTM C1072 bond wrench device, but the equation to calculate this value is the same for each.

Density Measurements

Density measurements are performed on cores taken from the grout samples after specimens have been broken. A wet coring drill is set up on a broken and elevated C1072 specimen to take a 2” core sample, as is shown in Figure 20 below.



Figure 20. Coring Drill Setup

Three core samples are taken from each grout batch to compare relative densities. ASTM C567 details the process for determining the equilibrium density, as well as an equation to use once all weights are obtained. After the core samples are acquired, they are allowed to soak in water for 24 hours. The apparent weight of the samples is then acquired by using a hanging scale suspended over the samples while they remain in water. The weight of the samples is also taken after being removed from the water and being patted dry with a paper towel, and finally the dried weight of the samples is acquired after they are allowed to stabilize in a humidity-controlled

environment. This environment is kept at a temperature of 23°C and a relative humidity of 50%. The specimens remain in this environment until the weight changes no less than 0.5% after successive measurements. When all weights are acquired, the equilibrium density is found using Equation 7 shown below.

$$E_m(\text{Density, kg/m}^3) = (A \times 997)/(B - C) \quad (1)$$

$$E_m(\text{Density, [lb/ft}^3]) = (A \times 62.3)/(B - C) \quad (2)$$

where:

- E_m = measured equilibrium density, kg/m³ [lb/ft³],
- A = mass of cylinder as dried, kg [lb],
- B = mass of saturated surface-dry cylinder, kg [lb], and
- C = apparent mass of suspended-immersed cylinder, kg [lb].

Equation 7. Equilibrium Density Formula

CHAPTER 6: RESULTS

Summary of Bond Wrench Results

The data gathered from bond wrench tests performed on fully grouted masonry specimens using Arcosa lightweight grout is laid out in this section. Table 8 shown below calculates the bond strength of these masonry specimens based on the resulting maximum force outputs from the tests. The equation to convert these force values into the resulting bond strength for the custom moment couple device is laid out in Equation 5 shown in Chapter 5. These bond strength values are compared to values for compression strength obtained from compression tests performed on C1019 grout samples within seven days of the flexural tensile strength bond wrench tests. The ratio shown in the sixth column of Table 8 consists of the bond strength divided by the compressive strength, multiplied into a percentage, which averages to 9.4%. This is to show how the compressive strength of these samples compares to their tensile strength, and this ratio is then compared to the same calculation for normal-weight samples.

Table 8. Tested Sample Strengths

Test Date	Breaking Strength	Applied Moment	Bond Strength	Compression Strength	Ratio	$f_r / \sqrt{f_g}$
	Applied P (lb)	M (lb*in)	f_r (psi)		f_r/f_g (%)	
6/29/2022 (Arcosa Batch 1)	717.8	26828.1	174.70	2015	8.7	3.9
7/15/2022 (Arcosa Batch 1)	702.0	26236.1	170.79	2015	8.5	3.8
8/3/2022 (Arcosa Batch 2)	976.6	36499.2	238.58	2602	9.2	4.7
8/4/2022 (Arcosa Batch 2)	1093.4	40864.6	267.41	2602	10.3	5.2
8/5/2022 (Arcosa Batch 2)	1101.5	41169.9	269.43	2602	10.4	5.3
				Average	9.4	4.6
				Standard Deviation	0.8	0.6

The $\frac{f_r}{\sqrt{f_g}}$ calculation shown in Table 8 is included to compare to the standard value from ACI 318, which specifies that $f_r = 7.5\sqrt{f_g}$. To compare to normal-weight grout based on this code, $\frac{f_r}{\sqrt{f_g}}$ should equal ~ 7.5 . However, this value was found to be 4.6 for the lightweight grout

samples. This calculation was also performed for the normal-weight grout data from previous studies to account for the fact that the 7.5 factor is for samples made up of solely grout, while these bond wrench tests include the full assembly and account for the strength of the mortar joint. Therefore, with these calculations performed for both normal-weight and lightweight samples, a more direct comparison could be made, with an expectation of a lower value than 7.5 due to the mortar assembly. Table 8 also shows the standard deviations for the ratio calculation and the $\frac{f_r}{\sqrt{f_g}}$ equation, both of which are low as all values are close to the overall mean.

Table 9. Predicted Strength

Test Date	Mortar Type	402-602 Predicted Bond Strength	Ratio
		f_{rp} (psi)	f_r/f_{rp}
6/29/2022 (Arcosa Batch 1)	Type S Mortar Cement	163	1.1
7/15/2022 (Arcosa Batch 1)		163	1.0
8/3/2022 (Arcosa Batch 2)		163	1.5
8/4/2022 (Arcosa Batch 2)		163	1.6
8/5/2022 (Arcosa Batch 2)		163	1.7
		Average	1.4

Table 10. Comparison between Bond Strength and Compression Stress

Test Date	Total Compression Force	Compression Stress	Bond Strength	Test Compression Stress / Bond Strength
	C (lb)	C_s (psi)	f_r (psi)	C_s / f_r (%)
6/29/2022 (Arcosa Batch 1)	296.4	2.5	223.75	1.42
7/15/2022 (Arcosa Batch 1)	296.4	2.5	218.77	1.46
8/3/2022 (Arcosa Batch 2)	296.4	2.5	305.14	1.04
8/4/2022 (Arcosa Batch 2)	296.4	2.5	341.88	0.93
8/5/2022 (Arcosa Batch 2)	296.4	2.5	344.45	0.92
			Average	1.16

Table 9 shows the comparison between the actual bond strength shown in Table 8 and the predicted bond strength from TMS 402-602. Because a Type S Mortar Cement was used for both lightweight grout mixes for this study, the predicted bond strength was 163 psi overall. This resulting average is 1.4. Table 10 compares the bond strength gathered from the flexural tensile strength tests conducted in this study and the compression stress for these tests. The displayed

compression force is based on the weights shown in Chapter 3 in Table 2. Overall, this resulted in an average ratio of 1.16% between compression stress and bond strength.

Table 11. Comparison to ASTM C1072-13 Bond Wrench Compression Stress

Minimum Predicted Bond Strength	Total Compression Force	ASTM Compression Stress	ASTM Compression Stress / Minimum Predicted Bond Strength
f_{rPmin} (psi)	C (lb)	C_s (psi)	C_s / f_{rPmin} (%)
51	44.15	1.6	3.13

Table 12. TMS 402-602 Predicted Bond Strengths for Various Mortar Types

Direction of flexural tensile stress and masonry type	Mortar types			
	Portland cement/lime or mortar cement		Masonry cement or air entrained portland cement/lime	
	M or S	N	M or S	N
Normal to bed joints				
Solid units	133 (919)	100 (690)	80 (552)	51 (349)
Hollow units ²				
UngROUTED	84 (579)	64(441)	51 (349)	31 (211)
Fully grouted	163 (1124)	158 (1089)	153 (1055)	145 (1000)
Parallel to bed joints in running bond				
Solid units	267 (1839)	200 (1379)	160 (1103)	100 (689)
Hollow units				
UngROUTED and partially grouted	167 (1149)	127 (873)	100 (689)	64 (441)
Fully grouted	267 (1839)	200 (1379)	160 (1103)	100 (689)
Parallel to bed joints in masonry not laid in running bond				
Continuous grout section parallel to bed joints	335 (2310)	335 (2310)	335 (2310)	335 (2310)
Other	0 (0)	0 (0)	0 (0)	0 (0)

¹ The values in this table shall not be applicable to structural clay tile unit masonry (ASTM C34, ASTM C56, ASTM C126, ASTM C212)

² For partially grouted masonry, modulus of rupture values shall be determined on the basis of linear interpolation between fully grouted hollow units and ungrouted hollow units based on amount (percentage) of grouting.

Table 11 shows this same data as gathered from the ASTM standard bond wrench test using a low-strength mortar cement. The compression force shown in this table is based on the standard weights of the bond wrench upper clamp and masonry specimen as detailed in ASTM C1072-13 and shown in Chapter 3 in Table 3, using a minimum predicted bond strength of 51 psi consistent with Type N masonry cement used on solid masonry prisms with applied load normal to the mortar joint. These standard predicted bond strength values are shown in Table 12 as per TMS 402-602. As can be seen, this resulted in an overall percentile ratio of compression stress to flexural tensile stress of 3.13%, somewhat higher than the value calculated from the lightweight grout tests using

our custom device. Therefore, it is assumed that the custom bond wrench device is more than sufficient with regards the ratio between compression strength and bond strength to be in a comparable stress state to normal-weight specimens tested with the ASTM C1072 device.

String Potentiometer Displacement Results

Shown below in Table 13 are the total displacements for the two string pots monitoring each side of the bond wrench device during each test. As can be seen, these displacements are similar between both devices for each test, apart from the test on July 15, 2022, in which String Pot 2 did not output correctly. However, these displacements show similar results overall and display that there were similar displacements for both sides of the bond wrench device during the testing process.

Table 13. Total Displacement of String Pots for Each Test

Test Date	String Pot Total Displacement	
	String Pot 1	String Pot 2
	SP1 (in)	SP2 (in)
6/29/2022 (Arcosa Batch 1)	0.696	0.755
7/15/2022 (Arcosa Batch 1)	0.373	0.044
8/3/2022 (Arcosa Batch 2)	0.503	0.383
8/4/2022 (Arcosa Batch 2)	0.671	0.682
8/5/2022 (Arcosa Batch 2)	0.423	0.389

Comparison of Data to Normal-Weight Specimens

The data gathered for lightweight grout from the flexural strength tests was subsequently compared to data for normal-weight grout gathered from existing research; this data is compiled in Table 13 below, showing results from four different studies. The ratio shown in column four displays the percentage ratio between the bond strength and compressive strength for these normal-weight samples. At the bottom of this table are shown average values for both the total amount of

data and solely for data within a comparable compressive strength range. The comparable compressive strength range is defined as values for compressive strength between 1987 psi and 3350 psi, as the compression strengths for the lightweight grout samples ranged from 2000 to 3000 psi. As can be seen, the tension/compression strength ratio for the comparable values is 10.2%, displaying a very similar result to the 9.4% from the lightweight grout. The 5.6% result from the total average of all normal-weight grout samples is much lower due to the high compression strength values of some of the results as compared to their overall lower bond strengths.

The $\frac{f_r}{\sqrt{f_g}}$ values were calculated for these normal-weight grout results as well in the same manner as the previously discussed ratio, calculating a value for all results, as well as a value solely for results with comparable compression strength values. For the total average, the normal-weight grout showed a result of 3.4, somewhat lower than the 4.6 value from the lightweight grout data. However, when taking an average from the results with comparable compression strengths, this average comes out to be 5.3, much closer to the lightweight grout's 4.6 result. This comparison between the bond strength and compression strength of both the lightweight and normal-weight samples is also shown graphically in Figure 21. As can be seen, the lightweight aggregate displays similar strengths when compared to normal-weight samples within the same range of compression strengths, while the results with higher compression strengths can be seen in the rightmost portion of the graph.

Table 14. Normal-Weight Grout Test Results

Research Study	Bond Strength	Compression Strength	Ratio	$f_r / \sqrt{f'_g}$	Mortar Type	TMS 402-602 Predicted Strength	Ratio
	f_r (psi)	f'_g (psi)	f_r/f'_g (%)			f_{rp} (psi)	f_r/f_{rp}
Brown & Melander, 1999	132	6192	2.1	1.7	Type N Masonry Cement	145	0.9
	122	6192	2.0	1.6		145	0.8
	137	6192	2.2	1.7		145	0.9
	132	6192	2.1	1.7		145	0.9
	141	6192	2.3	1.8		145	1.0
	162	6192	2.6	2.1		153	1.1
	152	6192	2.5	1.9	Type S Masonry Cement	153	1.0
	143	6192	2.3	1.8		153	0.9
	148	6192	2.4	1.9		153	1.0
	127	6192	2.1	1.6		153	0.8
	143	6192	2.3	1.8	Type N PCL	158	0.9
	152	6192	2.5	1.9		158	1.0
	138	6192	2.2	1.8		158	0.9
	144	6192	2.3	1.8		158	0.9
	148	6192	2.4	1.9		158	0.9
	154	6192	2.5	2.0		163	0.9
	154	6192	2.5	2.0	Type S PCL	163	0.9
	151	6192	2.4	1.9		163	0.9
	154	6192	2.5	2.0		163	0.9
	162	6192	2.6	2.1		163	1.0
Hamid & Drysdale, 1988	203.1	3060	6.6	3.7	Type S PCL	163	1.2
	197.3	1987	9.9	4.4		163	1.2
	242.2	5946	4.1	3.1		163	1.5
Hamid et al., 1992	300	2980	10.1	5.5	Type M/S PCL	163	1.8
	330	2980	11.1	6.0		163	2.0
	334	2980	11.2	6.1		163	2.0
	345	2980	11.6	6.3		163	2.1
	293	2980	9.8	5.4		163	1.8
	337	2980	11.3	6.2		163	2.1
Hamid et al., 1979	220	2080	10.6	4.8	Type S PCL	163	1.3
	300	3350	9.0	5.2		163	1.8
	500	5350	9.3	6.8		163	3.1
	220	2080	10.6	4.8		163	1.3
	220	2080	10.6	4.8		163	1.3
	500	5350	9.3	6.8		163	3.1
	500	5350	9.3	6.8		163	3.1
		Total Average	5.6	3.4		Total Average	1.4
		Average for Comparable f'_g	10.2	5.3		Average for Comparable f'_g	1.7

The ratio between the tested and predicted bond strengths were also calculated for the normal-weight samples, as is shown in column 8 of Table 14. For the total average of all results, this value was 1.4, while for the average of the results with comparable compression strengths, it was 1.7. This value is very close to the average value from the lightweight grout samples of 1.4, displaying a similarity in their overall effectiveness. The predicted strengths for these normal-weight grouts differ based on the type of mortar used, as per TMS 402-602.

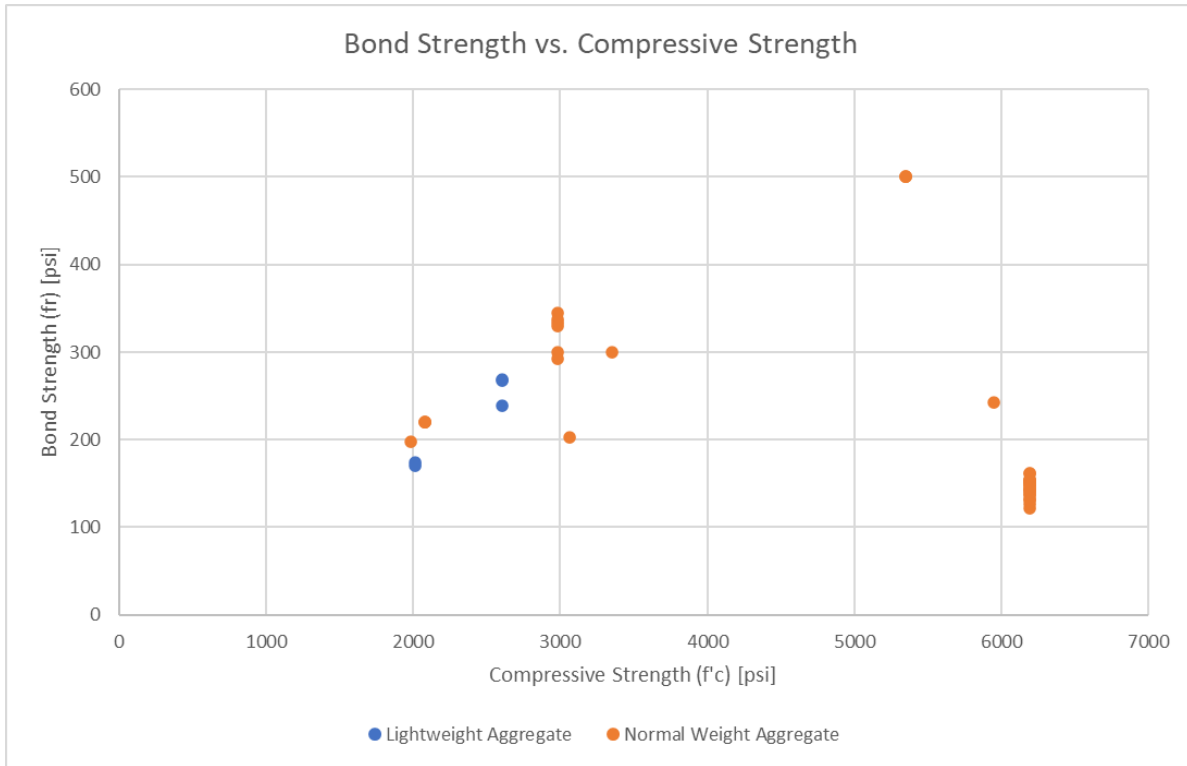


Figure 21. Lightweight vs. Normal-Weight Aggregate Bond Strength

Comparison to Modulus of Rupture Testing

The study “Behavior of Anchor Bolts in Concrete Masonry with Lightweight Grout,” by Shrestha et. al. (2022), was examined to determine how the strengths of various lightweight grout mixes as obtained through anchor bolt testing compared to the strengths for expanded clay grout gathered through bond wrench flexural tensile strength testing performed in this study. As can be seen in Table 15 below, the ratio between bond strength and compressive strength is slightly higher overall than the data gathered from the custom moment couple tests and from the literature for normal-weight concrete covered in Table 14. However, the data for the lightweight concrete material is closest overall to that of the above data, at 12.1% as compared to the 9.4% for the Arcosa lightweight grout. The value for $\frac{f_r}{\sqrt{f_g}}$ is higher than expected from ACI 318, and higher than that of the lightweight or normal-weight grout, being at 8.3 as compared to 4.6.

Table 15. Lightweight Concrete and Grout Results (Shrestha et al. 2022)

Material Type	Bond Strength Average	Compression Strength Average	Ratio	$f_r/\sqrt{f_g}$
	f_r (ksi)	f_g (ksi)	f_r/f_g (%)	
Lightweight Concrete	588.6	5389.2	10.9	8.0
Lightweight Grout	579.4	4245.1	13.6	8.9
Expanded Clay Grout	616.6	3374.5	18.3	10.6
Expanded Slate Grout	810.1	5122.6	15.8	11.3

Conclusion

Based on the data gathered for this study and its comparison to previous studies on both normal-weight and lightweight grout, it can be assumed that the bond strength values predicted by TMS 402-602 are appropriate for lightweight specimens, as they result in comparable ratios to normal-weight specimens, being 1.4 for lightweight grout and 1.7 for normal-weight grout, when compared based on similar compression strengths. This extends to the comparison between the values of $\frac{f_r}{\sqrt{f_g}}$ for both normal-weight and lightweight grout, as the lightweight grout gives a value of 4.6 as compared to 5.3 for normal-weight grout, based on using averages of only specimens with comparable compression strengths. Compared to the total dataset of normal weight specimens in the literature, the results of the lightweight grout, are better than or equivalent to these findings. These results as a whole are shown below in Table 16. Based on these results, there is no need to use a dedicated reduction factor for lightweight grout, as it produces strengths that are comparable to normal-weight grout and could be used in similar applications.

Table 16. Summarized Conclusions

	Ratio	$f_r / \text{sqrt}(f_g)$	Ratio
	f_r/f_g (%)		f_r/f_{rP}
Lightweight Grout	9.4	4.6	1.4
Normal-Weight Grout (Similar Compressive Strength)	10.2	5.3	1.7
Normal-Weight Grout (All Data)	5.6	3.4	1.4

Data Collection for Density-Based Lambda Reduction Factors

The final portion of this project consists of finding reduction factors for lightweight grout based on density. This was done by taking core samples from the lightweight grout used in the bond wrench tests, and finding various weights as detailed in Equation 6 below to find their equilibrium densities. Table 17 shows the three values needed for this calculation, the dried mass, the saturated surface-dry mass, and the apparent mass of the cylinder while suspended in water. The dried mass was taken by recording periodic measurements every 28 days on core samples in a humidity-controlled chamber until their mass changed no more than 0.5% between two successive measurements.

$$E_m(\text{Density, kg/m}^3) = (A \times 997)/(B - C) \quad (1)$$

$$E_m(\text{Density, [lb/ft}^3]) = (A \times 62.3)/(B - C) \quad (2)$$

where:

- E_m = measured equilibrium density, kg/m³ [lb/ft³],
- A = mass of cylinder as dried, kg [lb],
- B = mass of saturated surface-dry cylinder, kg [lb], and
- C = apparent mass of suspended-immersed cylinder, kg [lb].

Equation 6. Equilibrium Density

Table 17. Grout Density Measurements

Grout Batch	Sample Number	Sample Length (in)	Dried Mass (A) [lb]	SSD Mass (B) [lb]	Apparent Mass (C) [lb]	Equilibrium Density [lb/ft ³]	Avg. Equilibrium Density [lb/ft ³]
Arcosa 1	1	4.9375	0.81	0.93	0.28	77.8	77.2
	2	3.125	0.49	0.55	0.16	78.0	
	3	2.375	0.39	0.44	0.12	76.0	
	1 & 2	-	1.29	1.5	0.46	77.5	
	2 & 3		0.87	1.01	0.27	73.4	
	Arcosa 2	1	5.75	0.92	1.1	0.34	
2		5.4375	0.86	0.99	0.28	75.5	
3		3.4375	0.56	0.66	0.2	75.5	
1 & 2		-	1.79	2.09	0.55	72.4	
2 & 3			1.42	1.63	0.48	77.0	

Table 18. Dried Mass Measurements

Grout Batch	Sample Number	Sample Length (in)	Initial Measurement (grams)	Measurement 1 (grams)	Percent Difference	Measurement 2 (grams)	Percent Difference
			8-Sep-22	30-Sep-22	Initial to Measurement 1	28-Oct-22	Measurement 1 to 2
Arcosa 1	1	4.9375	423.7	378	11.4	368	2.7
	2	3.125	252.9	224	12.1	221.5	1.1
	3	2.375	199.3	179	10.7	177	1.1
	1 & 2	-	677.5	602	11.8	587	2.5
	2 & 3		455	403.5	12.0	395.5	2.0
Arcosa 2	1	5.75	491.8	432	12.9	419.5	2.9
	2	5.4375	448.5	401	11.2	390.5	2.7
	3	3.4375	292.9	261	11.5	253	3.1
	1 & 2	-	940	834	12.0	812	2.7
	2 & 3		742	663	11.2	645	2.8
			Average		11.7	Average	2.4

As per the second measurement, these values changed by an average of 2.4%, still outside of the acceptable range for the dried mass measurements, as can be seen in Table 18. However, these values were still used to calculate an intermediate equilibrium density for this most recent measurement. Based on Equation 6, these equilibrium densities were calculated as 77.2 lb/ft³ for Arcosa Batch 1 and 75.6 lb/ft³ for Arcosa Batch 2. These density measurements would require similar results from a different grout batch for comparison purposes in order to be useful for creating reduction factors based on density. Therefore, this portion of the study is still considered ongoing work. However, being able to create these density reduction factors would be ideal as current ACI codes base reduction factors on density rather than bond strength as detailed in the study above.

CHAPTER 7: CONCLUSION

This study covered the implementation of expanded clay lightweight aggregate (Arcosa) in masonry grout mixtures to be used in fully grouted masonry construction specimens. The flexural tensile strengths of these samples were found using a moment couple device modified from ASTM C1072-13 to accommodate the larger size of the C1072 samples. Firstly, other literature was examined to determine the previously studied benefits of lightweight concrete and lightweight grout, and to examine the viability of lightweight aggregate as a construction material. The custom moment couple test device was examined in terms of its overall construction and modifications that were required for it to function properly, and the capacity of each component was calculated to ensure the device would operate correctly. The design of the C1072 specimens was covered, including the procedure to construct them and then prepare them for testing in the moment couple device. This consisted of drilling holes for threaded rods and attaching metal plates to be used as attachment points for the bolts and angles on the bond wrench. The test procedure was covered in detail, going over each step to break one of the C1072 specimens correctly, and noting values and circumstances to be wary of for safety reasons. Finally, data was obtained for the flexural bond strength of these specimens. It was found that the lightweight grout masonry specimens exhibited ratios between tensile and compression strength in the same range as normal-weight grout specimens. Specifically, the lightweight grout specimens had an average $\frac{f_r}{\sqrt{f_g}}$ value of 4.6 compared to 5.3 for normal-weight grout of similar compression strength and 3.4 for the entire dataset of normal weight specimens.

Based on these results, it was determined that reduction factors for lightweight grout were unnecessary for flexural tension strength with tension normal to the bed joint. So, for this capacity

check using current TMS 402/602 tabulated values would be sufficient. Ultimately, this work contributes to building up the database of test results needed to formulate a design procedure and applicable reduction factors for TMS 402/602 equations where needed. If these changes were put into effect, it would result in a significant reduction in overall structure weight, as well as the increased thermal conductivity and water resistance exhibited by lightweight grout as examined by other researchers in the field.

REFERENCES

- ASTM C127, 2015, “Standard Test Method for Relative Density (Specific Gravity) and Absorption of Coarse Aggregate,” ASTM International, West Conshohocken, PA, 2015, DOI: 10.1520/C0127-15, www.astm.org
- ASTM C138, 2017, “Standard Test Method for Density (Unit Weight), Yield, and Air Content (Gravimetric) of Concrete,” ASTM International, West Conshohocken, PA, 2017, DOI: 10.1520/C0138_C0138M-17A, www.astm.org
- ASTM C567/C567M - 19, 2019, “Standard Test Method for Determining Density of Structural Lightweight Concrete,” ASTM International, West Conshohocken, PA, 2005, DOI: 10.1520/C0567_C0567M-19, www.astm.org
- ASTM C1072 – 13, 2019, “Standard Test Methods for Measurement of Masonry Flexural Bond Strength,” ASTM International, West Conshohocken, PA, 2019, DOI: 10.1520/C1072-19, www.astm.org
- ASTM E518, 2010, “Standard Test Methods for Flexural Bond Strength of Masonry,” ASTM International, West Conshohocken, PA, 2010, DOI: 10.1520/E0518-03, www.astm.org
- Bane, Dillon K. *Material and Structural Properties of Lightweight Masonry Grout*. ProQuest Dissertations Publishing, 2016.
- Bentz, Dale P., et al. *Influence of Internal Curing on Properties and Performance of Cement-Based Repair Materials*. U.S. Dept. of Commerce, National Institute of Standards and Technology, 2015.
- Bentz, D. and Weiss, W.. “Internal Curing: A 2010 State-of-the-Art Review. U.S. Department of Commerce.” National Institute of Standards and Technology. Gaithersburg, MD, 2011.
- Brown, Russell H., and John Melander. “Flexural Bond Strength of Unreinforced Grouted Masonry Using PCL and MC Mortars.” *Proceedings, the Eighth North American Masonry Conference*, Austin, Texas, June 6-9, 1999 [electronic Resource], 1999, p. 12 pages–12 pages.
- Cavalline, Tara L., et al. “Impact of Lightweight Aggregate on Concrete Thermal Properties.” *ACI Materials Journal*, vol. 114, no. 6, 2017, pp. 945–56, <https://doi.org/10.14359/51701003>.

Choi, Se-Jin, et al. "Direct Tensile Strength of Lightweight Concrete with Different Specimen Depths and Aggregate Sizes." *Construction & Building Materials*, vol. 63, 2014, pp. 132–41, <https://doi.org/10.1016/j.conbuildmat.2014.04.055>.

HAMID, AHMAD ABDEL. *BEHAVIOUR CHARACTERISTICS OF CONCRETE MASONRY*. ProQuest Dissertations Publishing, 1978.

Hamid, Ahmed A., and Robert G. Drysdale "Behavior of Concrete Block Masonry Under Axial Compression." *Journal of the American Concrete Institute*, vol. 76, no. 6, 1979, <https://doi.org/10.14359/6965>.

Hamid, Ahmed A., and Robert G. Drysdale. "Flexural Tensile Strength of Concrete Block Masonry." *Journal of Structural Engineering (New York, N.Y.)*, vol. 114, no. 1, 1988, pp. 50–66, [https://doi.org/10.1061/\(ASCE\)0733-9445\(1988\)114:1\(50\)](https://doi.org/10.1061/(ASCE)0733-9445(1988)114:1(50)).

Hamid, Ahmad A., et al. "Flexural Tensile Strength of Partially Grouted Concrete Masonry." *Journal of Structural Engineering (New York, N.Y.)*, vol. 118, no. 12, 1992, pp. 3377–92, [https://doi.org/10.1061/\(ASCE\)0733-9445\(1992\)118:12\(3377\)](https://doi.org/10.1061/(ASCE)0733-9445(1992)118:12(3377)).

Liu, Yang, et al. "Size Effect on Tensile Strength of Lightweight Aggregate Concrete: A Numerical Investigation." *Construction & Building Materials*, vol. 323, 2022, p. 126541–, <https://doi.org/10.1016/j.conbuildmat.2022.126541>.

Polanco, Hannah Jean. *Structural Lightweight Grout Mixture Design*. ProQuest Dissertations Publishing, 2017.

Rashad, Alaa M. "Lightweight Expanded Clay Aggregate as a Building Material – An Overview." *Construction & Building Materials*, vol. 170, 2018, pp. 757–75, <https://doi.org/10.1016/j.conbuildmat.2018.03.009>.

Rikli, Daniel. *Comparing Strength and Modulus of Elasticity Values for Prisms Constructed with Lightweight and Normal Weight Grout*. ProQuest Dissertations Publishing, 2020.

Shrestha, Rumi, et al. "Behavior of Anchor Bolts in Concrete Masonry with Lightweight Grout." *ACI Structural Journal*, 2022

Shrestha, Rumi, "Development of Lambda Factors for Masonry Design with Lightweight Grout" (2021). All Theses. 3689. https://tigerprints.clemson.edu/all_theses/3689

Shrestha, R., Redmond, L., and Thompson, J., "Diagonal Tensile Strength and Lap Splice Behavior of Concrete Masonry Assemblies with Lightweight Grout," *Construction and Building Materials*, 344, 2022.

Tanyildizi, Harun, and Ahmet Coskun. "The Effect of High Temperature on Compressive Strength and Splitting Tensile Strength of Structural Lightweight Concrete Containing Fly Ash." *Construction & Building Materials*, vol. 22, no. 11, 2008, pp. 2269–75, <https://doi.org/10.1016/j.conbuildmat.2007.07.033>.

APPENDIX I: SPECIMEN PREPARATION

1. Lay completed C1072 specimen on their side with blocks supporting each end. Make sure that the bottom of the plate is aligned with the bottom of the masonry and square.
2. Clamp ½" steel plate with holes to one masonry block face to serve as a guide for drilling pilot holes



Figure 22. Steel Plates Clamped to C1072 Specimen

3. Drill six pilot holes using 3/8" hammer drill bit to a depth of approximately 0.5" following guide of plate
4. Repeat steps 2-3 for other block face
5. Remove steel plates and drill final holes using ½" hammer drill bit to a depth of 2.5" Make sure holes are 90 degrees to the face of the masonry (straight).

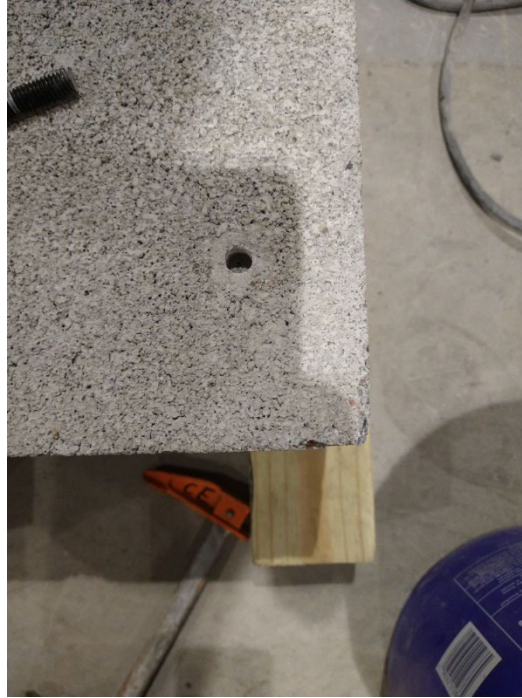


Figure 23. Drilled Hole in C1072

6. Use a vacuum with funnel attachment to remove excess dust from inside and around each hole

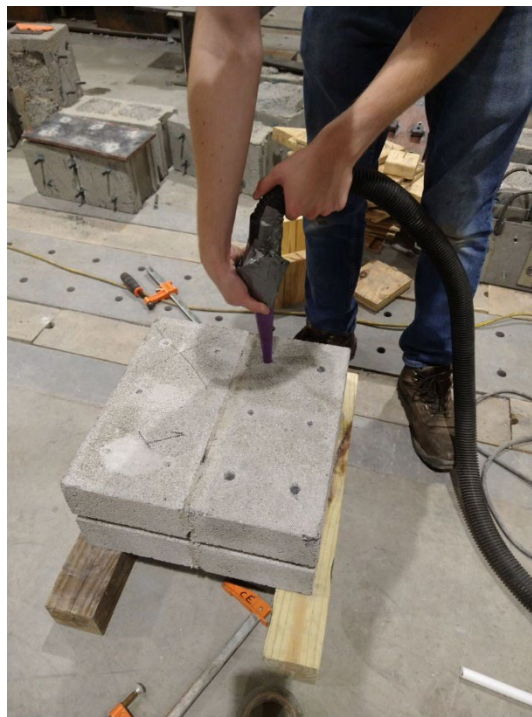


Figure 24. Drilled Holes being Vacuumed

7. Use piece of threaded rod with 2.5" length marked to check that hole is to correct depth



Figure 25. Threaded Rod in Drilled Hole

8. Repeat steps 1-6 for other side of C1072
9. Take tube of opened SET-XP epoxy with nozzle attached and insert into epoxy gun
10. Use epoxy gun to fill each drilled hole fully with epoxy
11. Insert 3.5" length 3/8" diameter threaded rod into each hole until it bottoms out, displacing epoxy
12. Use paper towel to clean excess epoxy from around threaded rods such that there is no buildup on the surface of the masonry
13. Place pieces of wood as spacers on surface of masonry for placing steel plate, creating an elevated surface of approximately 1/2" high above the face of the masonry.
14. Place steel plate back onto masonry while resting on wood spacers
15. Line up plate with each protruding threaded rod such that all six holes are filled



Figure 26. Threaded Rod Lined Up with Steel Plates

16. Use wooden 90-degree angles to line up two outside corners of steel plate such that plate is aligned with outside of masonry. Clamp in place to allow the epoxy to dry.

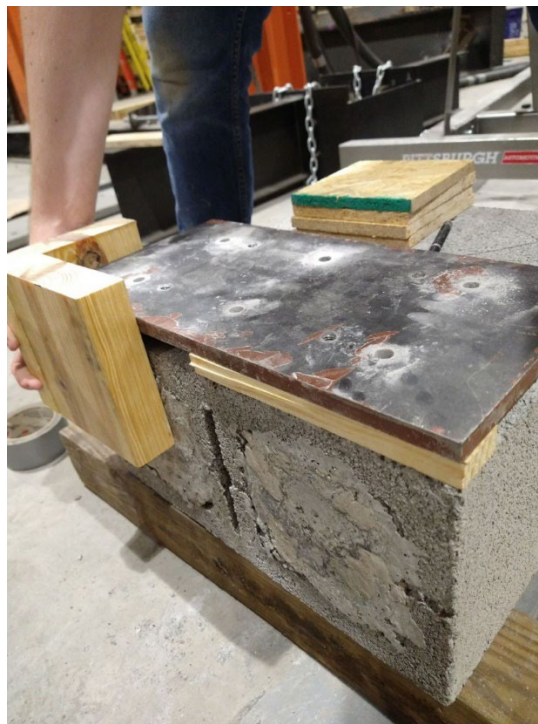


Figure 27. Steel Plates Being Aligned to C1072 Corners

17. Repeat steps 9-15 for other masonry block on face of C1072
18. Allow epoxy to set for 4-6 hours before removing steel plates from both block faces
19. Invert C1072 and repeat steps 9-16

APPENDIX II: TESTING PROCEDURE

Setup

1. Check that hydraulic pump has an adequate amount of fluid
2. Add blocks under left side of upper beam in case of any
3. Grease surface that actuators will be contacting with hydraulic fluid
4. Begin recording on DAQ and pressure gauge computer (video conference with portable cameras)
5. Check that valves are open for both outputs of hydraulic splitter
6. Plug in NI console into computer and turn on power supply and NI console
7. Open Clemson DAQ and open data acquisition program
8. Ensure that each device is inputting correctly by pulling on string pots
9. Do preliminary checks on a few devices to check that when string pots are moved, an equivalent displacement is shown on the DAQ reading
10. Make sure cameras are set up and in place for each pressure gauge and dial gauge
11. Plug in cords for all cameras
12. Set up screen recorder for cameras on zoom
13. Zero both pressure gauges

Safety Protocol

1. If specimen or bolts slip or move for any reason, stop testing and fix
2. If data output from acquisition devices begins showing incorrect readings, stop test so that they can be corrected
3. If loading beam begins to twist, immediately stop test and unload
4. Stop if there is a pressure differential between actuators
5. Stop if maximum pressure of 10,000 psi for actuators is approached
6. Stop if maximum pull-out force for bolts of 4200 psi is approached
7. Unload quickly by twisting valve on hydraulic pump

Test Procedure

Initial Contact

1. Begin operating hydraulic pump a few times
2. Check that both actuator cylinders are moving
3. Pump to 1-5% of expected masonry failure
3.1.15 - 76 psi
4. Check hydraulic hose connections for any leaks
5. Compare shown psi to lbs (multiply by 2.76 in²)
6. Operate hydraulic pump until actuator cylinders have contacted central beam
7. Zero both pressure gauges

Load to Failure

1. Begin operating hydraulic pump at consistent rate so that force is applied over a period of 1-3 minutes
2. While operating the pump, observe camera output for pressure gauges to ensure that pressure remains equal on both sides
3. Look at dial gauge feed to check that column members are not bending
4. Visually check at regular intervals that beam is not twisting
5. Check that displacement outputs are reading as beam begins to move
6. Check data acquisition software to ensure that displacement and force output on both sides of central specimen is the same or very similar
7. Continue checking data throughout the test to ensure that displacements are equal on both sides and match expected outputs from graphs
8. Check pressure gauge readings to check that force output on both sides is equal
9. Once specimen breaks, check final pressure output

Final Data Saving

1. Check and save peak displacements and force outputs from recorded data
2. Check that displacements and forces for both sides of specimen match
3. Make sure screen has been recorded for pressure gauge output
4. Record final breaking strength based on visual reading
5. DAQ Scribe file will be saved to DAQ Scribe folder on computer, and can be converted to excel file
6. After removing specimen from device, document the failure surface for the specimen with photos

APPENDIX III: CAPACITY CALCULATIONS

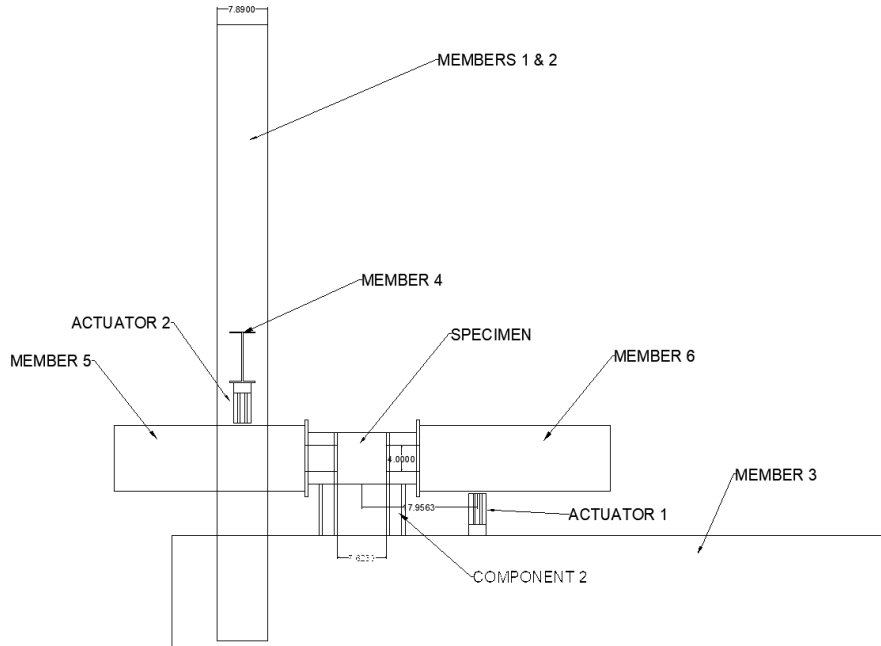


Figure 28. Diagram showing profile of Bond Wrench device

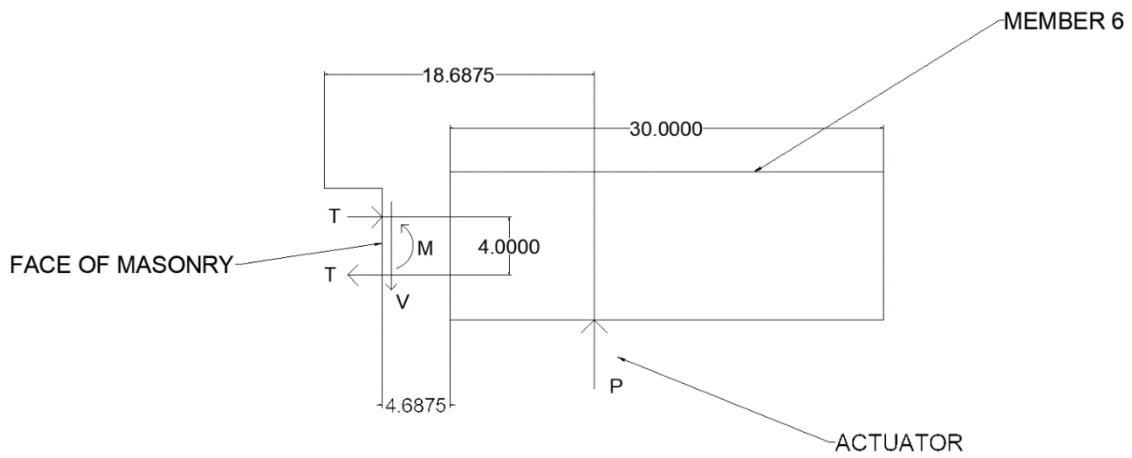


Figure 29. Load path for moment application to masonry

Initial Check on Upper Bound Expected Actuator Force Compared to Actuator Capacity

“INPUTS”	
“Compressive Strength”	$f_g := 3000 \text{ psi}$
“Compression Area”	$A := 15.625 \cdot \text{in} \cdot 7.625 \cdot \text{in} = 119.141 \text{ in}^2$
“Member Self-Weight”	$P_{SW} := \frac{19 \cdot \text{lb} \cdot \text{ft}}{\text{ft}} \cdot 30 \cdot \text{in} = 0.048 \text{ kip}$
“Modulus of Rupture”	$f_r := 0.6 \cdot \sqrt{\frac{f_g}{1000}} \cdot \text{ksi} = 1.039 \text{ ksi}$
<i>“Taken from Figure 8b in Tensile and Shear Behavior of Anchor Bolts”</i>	
“Full Moment Arm Length”	$L := 2 \cdot 18.6875 \cdot \text{in}$
“Compression Block Depth”	$c := 3.8125 \cdot \text{in}$
“Moment of Inertia”	$I := \frac{(15.625 \cdot \text{in}) (7.625 \cdot \text{in})^3}{12} = 577.243 \text{ in}^4$
“Member Length”	$L_{mem} := 30 \cdot \text{in}$
“Screw Gap Length”	$L_{gap} := 4.6875 \cdot \text{in}$
“OUTPUTS”	
“Maximum Stress”	$\sigma := f_r = 1.039 \text{ ksi}$
“Moment”	$M := \frac{I}{c} \cdot \left(\sigma + \frac{2 \cdot P_{SW}}{A} \right) = 157.468 \text{ kip} \cdot \text{in}$
“Individual Actuator Output”	$P := \frac{M}{L} = 4.213 \text{ kip}$
“Maximum Actuator Output for RCH121”	$P_{max} := 27.6 \cdot \text{kip}$

Check on Threaded Rod and Nuts to Attach the Specimen to the Plate

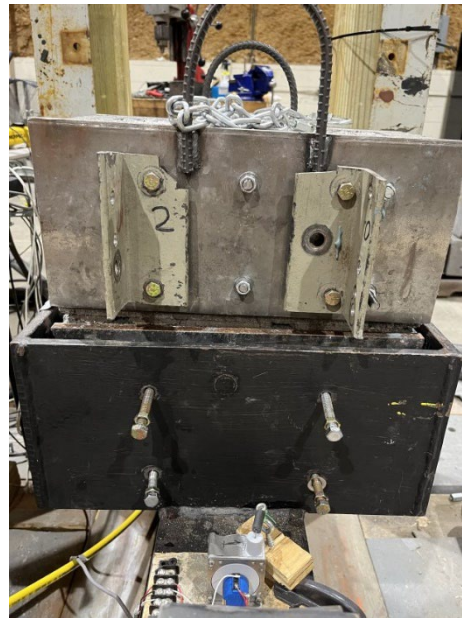


Figure 30. C1072 specimen in Bond Wrench attached to Member 3, 3 rods in each row, two rows per steel plate

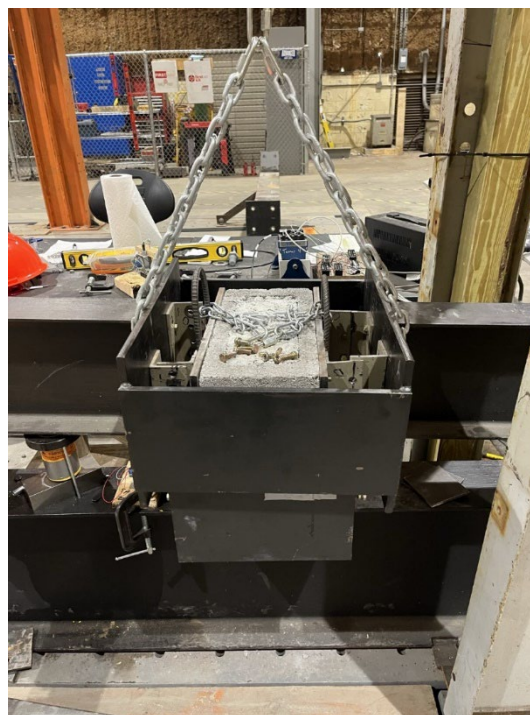


Figure 31. C1072 specimen installed in Bond Wrench and connected to Member 6

“Threaded Rod Strength (Grade B7_B16)_Attached to Masonry” “ASTM A193”



“Yield Strength” $Y := 105 \cdot ksi$

“Bolt Area” $A_b := 0.0775 \cdot in^2$

“Bolt Capacity” $T_{bolt} := Y \cdot A_b = 8.138 \text{ kip}$

“Appropriate Bolt to Exceed Tension Capacity_SAEJ995_Gr8”



$SAE_J995_Gr8_Nut_ProofLoad := 11.625 \cdot kip$

8	Medium carbon or alloy steel, quenched & tempered	1/4 – 5/8	150,000	C24	C32		
		Over 5/8 – 1		C26	C34		
		Over 1 – 1 1/2		C26	C36		

(1): Zinc coating refers to nuts that have been plated with a plating or coating of sufficient thickness to

“Masonry Screw Capacities”

$T_{cap} := T_{bolt}$

8	Medium carbon or alloy steel, quenched & tempered	1/4 – 5/8	150,000	C24	C32		
		Over 5/8 – 1		C26	C34		
		Over 1 – 1 1/2		C26	C36		

(1): Zinc coating refers to nuts that have been plated with a plating or coating of sufficient thickness to

“Theoretical Moment and Shear to break masonry”

“Embedment Depth = 2””

“Edge Distance = 2””

$$M_{th} := P \cdot \left(\frac{L}{2} - c \right) + P_{SW} \cdot \left(\frac{L_{mem}}{2} + L_{gap} \right) = 63.607 \text{ kip} \cdot in$$

“End Distance = 2””

“Spacing = 4””

$$V_{th} := P + P_{SW} = 4.261 \text{ kip}$$

$$S := 4 \cdot in$$

“Applied Tension Force”

$$T := \frac{M_{th}}{S} = 15.902 \text{ kip}$$

$$N_T := \frac{T}{T_{cap}} = 1.954$$

“Number of Screws Required for Tension”

“Applied Shear Force”

$$V := V_{th} = 4.261 \text{ kip}$$

“Shear per bolt”

$$v_{bolt} := \frac{V}{6} = 0.71 \text{ kip} \quad \text{“low, unlikely to be an issue”}$$

Check on Bolts from Member 6 to Plate on Masonry Specimen



Figure 32. Member 6 being put into place on the upper half of C1072

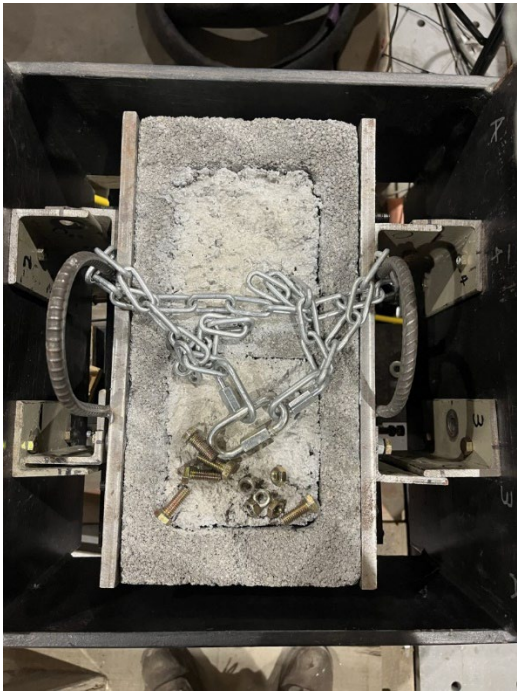




Figure 33. Angle connections between C1072 and Member 6

“Bolts to External Loading Arm: Tension, Shear, and Bending_Grade 8”



SAE J429-Grade 8	Medium carbon alloy steel: quenched & tempered	1/4 - 1 1/2	120,000	150,000	C33	C39	130,000	
SAE J429-Grade 8.2	Low carbon boron steel: quenched & tempered	1/4 - 1	120,000	150,000	C33	C39	130,000	

$$T_{proof_3_8_16_Gr8} := 9300 \text{ lbf}$$

$$Bolts_3_8_dia := \frac{3}{8} \cdot in$$

“Appropriate Nut to Exceed Tension Capacity_SAEJ995_Gr8”

$$SAE_J995_Gr8_Nut_ProofLoad := 11.625 \cdot kip$$

8	Medium carbon or alloy steel, quenched & tempered	1/4 – 5/8	150,000	C24	C32		
		Over 5/8 – 1		C26	C34		
		Over 1 – 1 1/2		C26	C36		

(1): Zinc coating refers to nuts that have been plated with a plating or coating of sufficient thickness to

“4 Grade 8 Bolts”

“Shear Capacity for Bolts (Grade 8)_Fully Threaded use Minor area”

$$V_{th} = 4.261 \text{ kip}$$

$$V_{su_Gr8} := 6 \text{ kip} \quad \text{“allowable shear stress for bolt material”}$$

<https://www.fastenal.com/en/84/load-calculator>

“ok”

“Tension Check”

$$T_U := \frac{M_{th}}{2 \cdot 4 \cdot in} = 7.951 \text{ kip} \quad T_{proof_3_8_16_Gr8} := 9300 \text{ lbf} \quad \text{“ok” } T_{proof_3_8_16_Gr8} > T_U$$

“1/2 factor accounts for two bolts”

“4 inch spacing”

“Tapped Hole Check_Grade 50_Plate”

$$F_{y_plate} := 50 \text{ ksi}$$

$$\text{Tapped_Thickness} := 0.5 \text{ in}$$



Minimum Thread Engagement (Bolt Failure) Chart – Standard

Coarse Threads

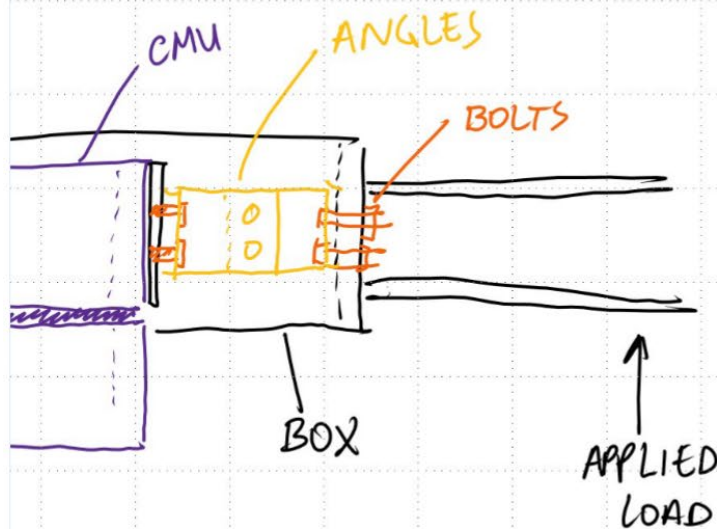
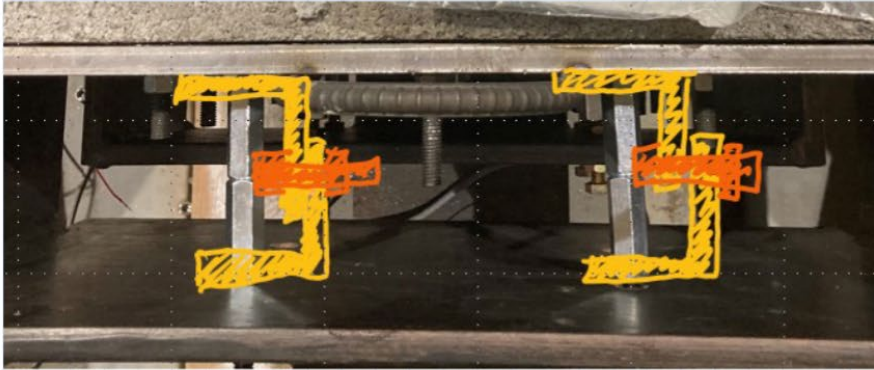
Thread Size	Nominal Diameter (in)	Stress Area (in ²)	Nut Material: Low Carbon Steel Yield Strength (ksi): 48			Nut Material: Nodular Iron Yield Strength (ksi): 52.5			Nut Material: A356-T6 Yield Strength (ksi): 24		
			Grade 2	Grade 5	Grade 8	Grade 2	Grade 5	Grade 8	Grade 2	Grade 5	Grade 8
			(in)	(in)	(in)	(in)	(in)	(in)	(in)	(in)	(in)
1/4 - 20	0.250	0.0318	0.14	0.23	0.29	0.13	0.21	0.27	0.29	0.47	0.58
5/16 - 18	0.313	0.0524	0.19	0.31	0.38	0.17	0.28	0.35	0.38	0.61	0.77
3/8 - 16	0.375	0.0775	0.23	0.38	0.47	0.21	0.35	0.43	0.47	0.76	0.95
7/16 - 14	0.438	0.1063	0.27	0.44	0.56	0.25	0.41	0.51	0.55	0.89	1.11
1/2 - 13	0.500	0.1419	0.32	0.52	0.65	0.29	0.47	0.59	0.64	1.04	1.30
5/8 - 11	0.625	0.2260	0.41	0.66	0.83	0.37	0.61	0.76	0.82	1.32	1.65
3/4 - 10	0.750	0.3340	0.50	0.82	1.02	0.46	0.75	0.93	1.01	1.63	2.04
7/8 - 9	0.875	0.4620	0.60	0.97	1.21	0.54	0.88	1.10	1.19	1.93	2.42
1 - 8	1.000	0.6060	0.68	1.11	1.39	0.63	1.01	1.27	1.37	2.22	2.77

“Bending Check Angle Option”

“Theoretical Moment and Shear to break masonry”

$$M_{th} := P \cdot \left(\frac{L}{2} - c \right) + P_{sw} \cdot \left(\frac{L_{mem}}{2} + L_{gap} \right) = 63.607 \text{ kip} \cdot \text{in}$$

$$M := M_{th} \cdot \frac{1}{2} = 31.803 \text{ kip} \cdot \text{in} \quad \text{“Moment per angle”}$$



“must connect angle to two bolts vertically to carry moment, bolts are 4” apart,”

“assumed a 5in angle length, 1/4in plate, A36 steel”

$$I := \frac{0.25 \text{ in} \cdot (5 \text{ in})^3}{12} = 2.604 \text{ in}^4$$

$$\sigma := M \cdot \frac{(2.5 \text{ in})}{I} = 30.531 \text{ ksi} \quad \text{"less than 36 ksi, we might have higher strength"}$$

"shear check"

$$V := \frac{V_{th}}{2} = 2.13 \text{ kip} \quad A_{plate} := 0.25 \text{ in} \cdot 5 \text{ in} = 1.25 \text{ in}^2$$

$$\tau_{max} := \frac{3 \cdot V}{2 \cdot A_{plate}} = 2.556 \text{ ksi}$$

"use grade 8 3/8-16 bolts"

$$T_{proof_3_8_16_Gr8} := 9300 \text{ lbf}$$

"Shear Capacity for Bolts (Grade 8)_Fully Threaded use Minor area"

$$V_{su_Gr8} := 6 \text{ kip} \quad \text{"allowable shear stress for bolt material"}$$

<https://www.fastenal.com/en/84/load-calculator>

"ok, exceeds V of 2.13 kip"

$$S := 4 \text{ in}$$

$$\text{"Applied Tension Force"} \quad T := \frac{M_{th}}{2 \cdot S} = 7.951 \text{ kip}$$

$$N_T := \frac{T}{T_{proof_3_8_16_Gr8}} = 0.855 \quad \text{"Number of Screws Required for Tension"}$$



Figure 34. Steel tube for connection between C1072 and Member 3

Check on Epoxy Anchor Capacity (Masonry Breakout)

“Anchor Pull-Out Check (Epoxy Capacity)”

“Compressive Strength” $f_g := 3500 \text{ psi}$

“Compression Area” $A := 15.625 \cdot \text{in} \cdot 7.625 \cdot \text{in} = 119.141 \text{ in}^2$

“Member Self-Weight” $P_{SW} := \frac{19 \cdot \text{lb} \cdot \text{ft}}{\text{ft}} \cdot 30 \cdot \text{in} = 0.048 \text{ kip}$

“Modulus of Rupture” $f_r := 0.15 \cdot f_g \cdot \text{psi} = 0.525 \text{ ksi}$

Revised to 15% of f_g based on initial testing (to determine true system limit)

“Full Moment Arm Length” $L := 2 \cdot 18.6875 \cdot \text{in}$

“Compression Block Depth” $c := 3.8125 \cdot \text{in}$

“Moment of Inertia” $I := \frac{(15.625 \cdot \text{in}) (7.625 \cdot \text{in})^3}{12} = 577.243 \text{ in}^4$

“Member Length” $L_{mem} := 30 \cdot \text{in}$

“Screw Gap Length” $L_{gap} := 4.6875 \cdot \text{in}$

“Maximum Stress” $\sigma := f_r = 0.525 \text{ ksi}$

“Moment” $M := \frac{I}{c} \cdot \left(\sigma + \frac{2 \cdot P_{SW}}{A} \right) = 79.61 \text{ kip} \cdot \text{in}$

“Individual Actuator Output” $P := \frac{M}{L} = 2.13 \text{ kip}$

$M_{th} := P \cdot \left(\frac{L}{2} - c \right) + P_{SW} \cdot \left(\frac{L_{mem}}{2} + L_{gap} \right) = 32.619 \text{ kip} \cdot \text{in}$
 “moment on one side of masonry”

$T := \frac{M_{th}}{S} = 8.155 \text{ kip}$ “Tension induced in each group of rods”

$T_{cap_unfactored} := 1.490 \text{ kip} \cdot 5 = 7.45 \text{ kip}$

SET-XP Allowable Tension and Shear Loads for Threaded Rod and Rebar in the Face of Fully Grouted CMU Wall Construction^{1, 3, 4, 5, 6, 8, 9, 10, 11}



Diameter (in.) or Rebar Size No.	Drill Bit Diameter (in.)	Minimum Embedment ² (in.)	Allowable Load Based on Bond Strength ⁷ (lb.)	
			Tension Load	Shear Load
Threaded Rod Installed in the Face of CMU Wall				
3/8	1/2	3 3/8	1,490	1,145
1/2	3/4	4 1/2	1,825	1,350
5/8	3/4	5 1/2	1,895	1,350
3/4	7/8	6 1/2	1,895	1,350
Rebar Installed in the Face of CMU Wall				
#3	1/2	3 3/8	1,395	1,460
#4	3/4	4 1/2	1,835	1,505
#5	3/4	5 1/2	2,185	1,505

1. Allowable load shall be the lesser of the bond values shown in this table and steel values, shown on p. 43.
2. Embedment depth shall be measured from the outside face of masonry wall.
3. Critical and minimum edge distance and spacing shall comply with the information on p. 38. Figure 2 on p. 38 illustrates critical and minimum edge and end distances.
4. Minimum allowable nominal width of CMU wall shall be 8". No more than one anchor shall be permitted per masonry cell.
5. Anchors shall be permitted to be installed at any location in the face of the fully grouted masonry wall construction (cell, web, bed joint), except anchors shall not be installed within 1 1/2" of the head joint, as show in Figure 2 on p. 38.
6. Tabulated allowable load values are for anchors installed in fully grouted masonry walls.
7. Tabulated allowable loads are based on a safety factor of 5.0.
8. Tabulated allowable load values shall be adjusted for increased base material temperatures in accordance with Figure 1 below, as applicable.
9. Threaded rod and rebar installed in fully grouted masonry walls are permitted to resist dead, live, seismic and wind loads.
10. Threaded rod shall meet or exceed the tensile strength of ASTM F1554, Grade 36 steel, which is 58,000 psi.
11. For installations exposed to severe, moderate or negligible exterior weathering conditions, as defined in Figure 1 of ASTM C62, allowable tension loads shall be multiplied by 0.80.

Note our embedment depth could not be 3 3/8" and was only 2 1/2"
Based on TMS 402-22 equations for cast-in-place anchors:

9.1.6.2.2 Anchor bolt nominal strengths used for design shall not exceed 65 percent of the average failure load from the tests.

Tensile breakout of cast in place masonry anchor bolts:

125,000 psi (8,618 MPa).

$$B_{anb} = 4A_{pt} \sqrt{f'_m} \quad \text{(Equation 9-1)}$$

To calculate Apt:

9.1.6.3.1 Axial Tensile Strength of Headed and Bent-Bar Anchor Bolts — Tensile strength of a headed anchor bolt is governed by breakout of an approximately conical volume of masonry starting at the anchor head and having a fracture surface oriented at approximately 45 degrees to the masonry surface, Equation 9-1, or by the tensile strength of the anchor steel, Equation 9-2.

Thus Apt is πR^2 , where $R = \text{embedment length} \cdot \tan(45)$

Thus anchor bolt conical breakout is proportional to embedment length²

Adjusting nominal unfactored capacity for reduced embedment length

$$ReductionFactor_EmbLength := \frac{2.5^2}{\left(3 + \frac{3}{8}\right)^2} = 0.549$$

$$T_{cap_factored} := T_{cap_unfactored} \cdot ReductionFactor_EmbLength = 4.088 \text{ kip}$$

$$T_{rod} := \frac{T}{2} = 4.077 \text{ kip}$$

Tension in each rod, only count 2 of 3 rods as the middle rod could not be emdeded in grout and is within the masonry web. Elected not to apply the additional 0.65 factor on top of this conservatism. (from TMS 402)

Based on this calculation, maximum grout strength for the device is approximately 3500 psi.

Check on Connections of Upper Actuator to Member 4

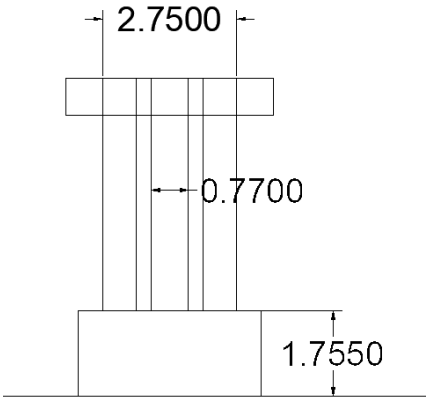


Figure 35. Actuator dimension diagram



Figure 36. Actuator 1 setup

“Moment developed in actuator attachment ring”

$$P = 4.213 \text{ kip} \quad \text{“Actuator Output”}$$

$$A := 0.0364 \cdot \text{in}^2 \quad \text{“Threaded rod area”}$$

$$d_1 := \frac{1.38}{2} \cdot \text{in} = 0.69 \text{ in} \quad \text{“Distance from CL to contact point”}$$

$$d_2 := \left(1 + \frac{15}{16}\right) \cdot \text{in} = 1.938 \text{ in} \quad \text{“Distance between attachment screws”}$$

$$M_1 := P \cdot d_1 = 2.907 \text{ kip} \cdot \text{in} \quad \text{“Total Moment”}$$

$$T_1 := \frac{M_1}{d_2} = 1.5 \text{ kip} \quad \text{“Tension required in screws”}$$

$$\sigma_1 := \frac{T_1}{A} = 41.221 \text{ ksi} \quad \text{“Stress from tensile load”}$$

“Check against stress capacity for bolt”

$$\sigma := \sigma_1 = 41.221 \text{ ksi} \quad \text{“Total stress in system”}$$

$$T_{cap} := 6.6 \cdot \text{kip} \quad \text{“1/4” Grade 8 bolt tension capacity”}$$

$$T_{rod_cap} := 2.18 \cdot \text{kip} \quad \text{“1/4” NF threaded rod capacity”}$$

BOLTS												
IDENTIFICATION · STRENGTH · CLAMP · TORQUE												
GRADE 2			* GRADE 5			GRADE 8						
Diameter	Proof Load	Yield Strength	Tensile Strength	Diameter	Proof Load	Yield Strength	Tensile Strength	Diameter	Proof Load	Yield Strength	Tensile Strength	
1/4-20	55,000	57,000	74,000	1/4-11	88,000	92,000	120,000	1/4-20	120,000	120,000	150,000	
3/8-16	53,000	56,000	72,000	3/8-16	74,000	81,000	118,000	3/8-16	120,000	120,000	150,000	
Low or medium Carbon Steel			Medium Carbon Steel, Quenched & Tempered			Carbon Alloy Steel, Quenched & Tempered			Carbon Alloy Steel, Quenched & Tempered			
SIZE	CLAMP LOAD ¹ Lbs	ASSEMBLY TORQUE	MINIMUM TENSILE STRENGTH Lbs	CLAMP LOAD ¹ Lbs	ASSEMBLY TORQUE	MINIMUM TENSILE STRENGTH Lbs	CLAMP LOAD ¹ Lbs	ASSEMBLY TORQUE	MINIMUM TENSILE STRENGTH Lbs	CLAMP LOAD ¹ Lbs	ASSEMBLY TORQUE	MINIMUM TENSILE STRENGTH Lbs
1/4-20	1320	66	50	2700	2000	8	75	4450	2850	12	9	6600
1/4-28	1500	76	56	2900	2300	10	86	4840	3250	14	10	7200

Tensile Strength (NF Threads)			
Size	TPI*	PSI**	Pounds
1/4	28	60,000	2180

$$\sigma_{max} := \frac{T_{cap}}{A} = 181.319 \text{ ksi} \quad \text{“Maximum allowable stress”}$$

$$\sigma_{max} > \sigma \quad \text{“OK”}$$

Summary

The epoxied anchors were determined to be the weakest part of the designed set up. Based on a compressive strength of 3500 psi for the grout, a force of 4.077 kips would be induced on each epoxy connection, nearly reaching their capacity. For this reason, it was determined that this epoxy connection was the limiting factor and that a grout mix with a compressive strength higher than 3500 psi could not be tested in this device.

APPENDIX IV: STRING POTENTIOMETER DISPLACEMENT GRAPHS

***Bold dot in graphs denote point of failure during test**

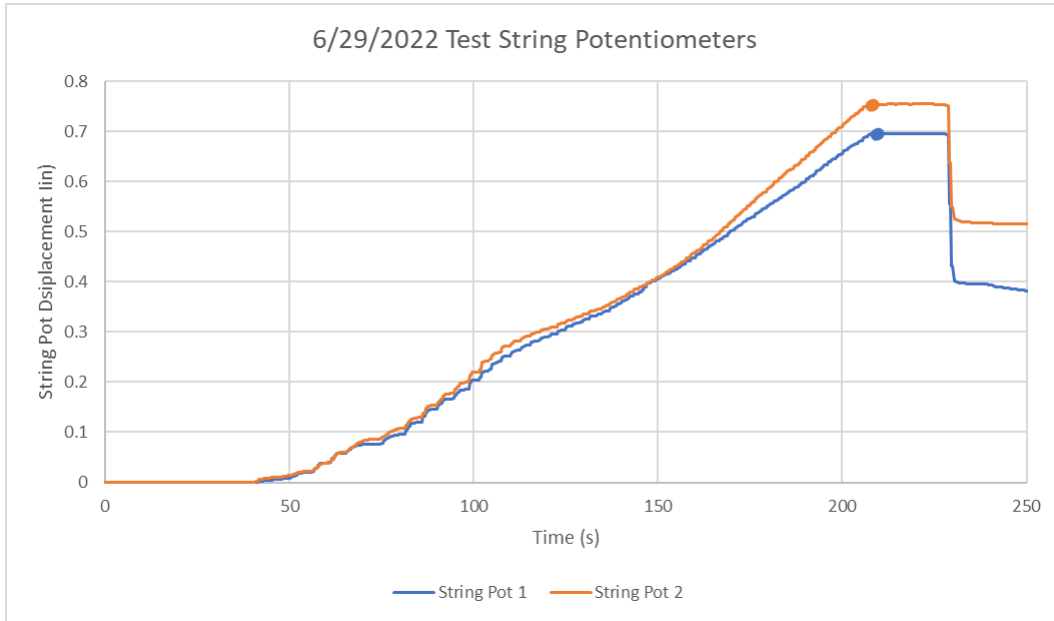


Figure 37. 6/29/2022 Test String Potentiometers

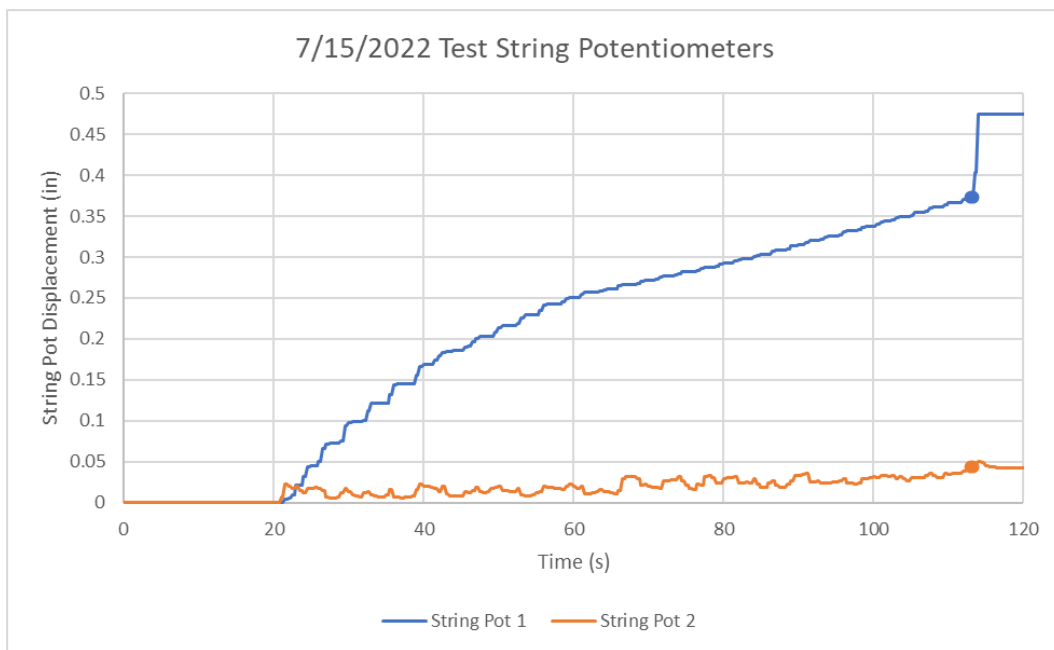


Figure 38. 7/15/2022 Test String Potentiometers

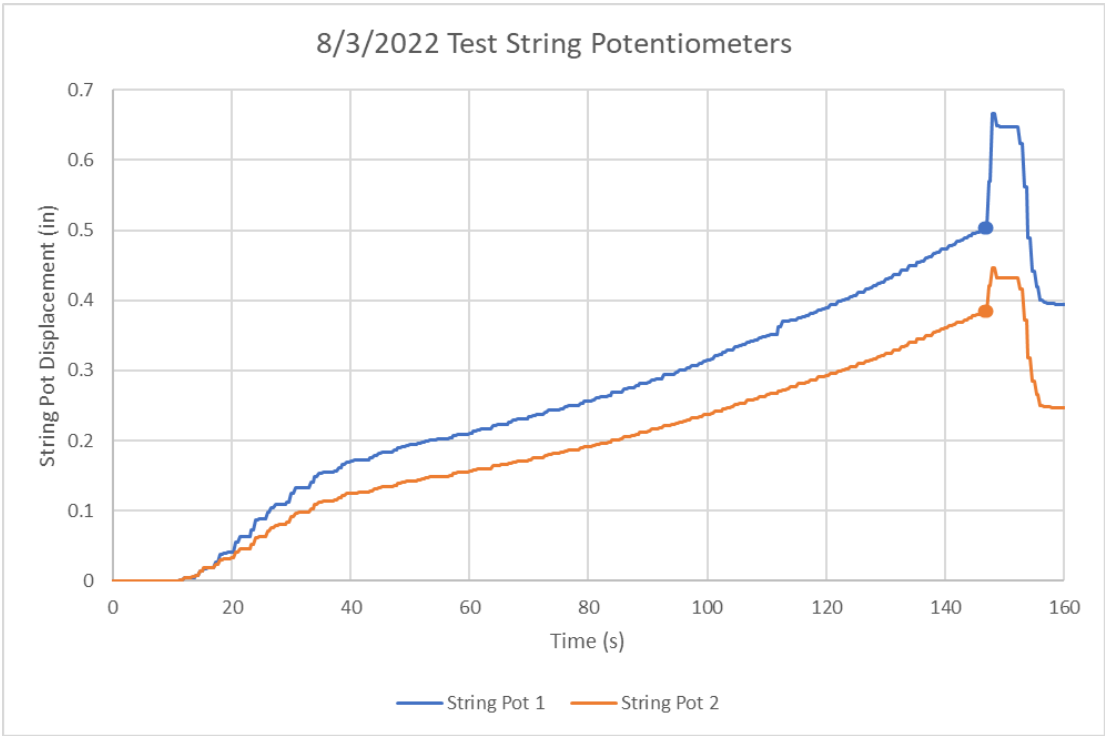


Figure 39. 8/3/2022 Test String Potentiometers

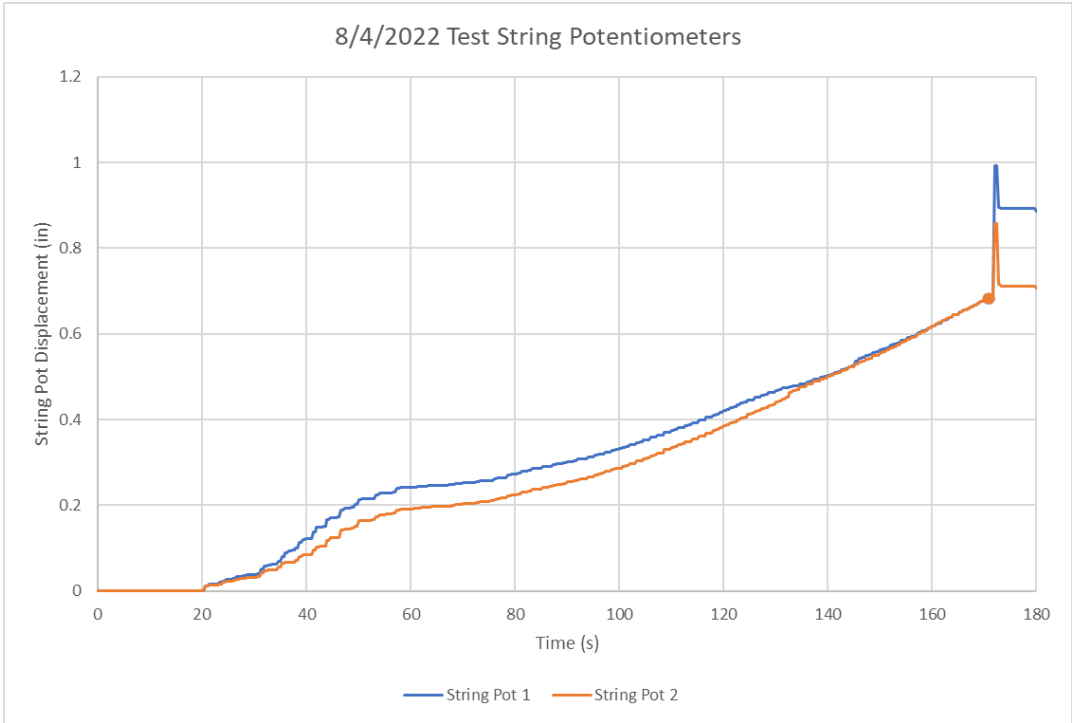


Figure 40. 8/4/2022 Test String Potentiometers

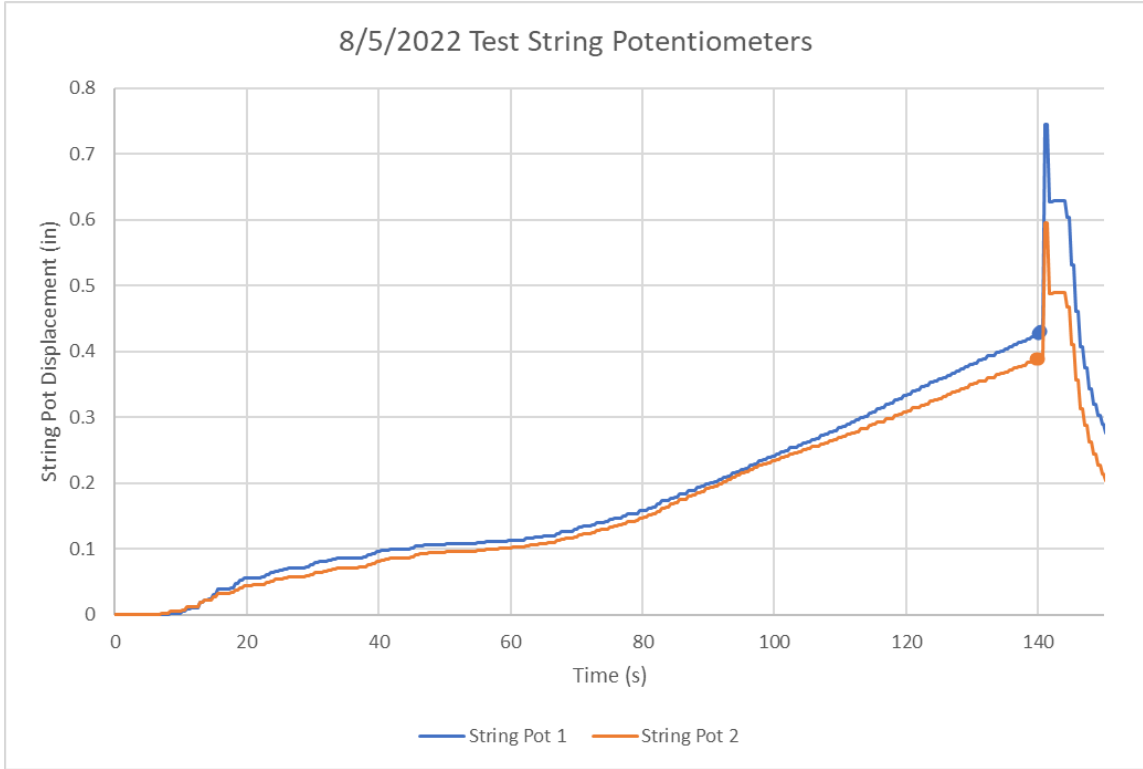


Figure 41. 8/5/2022 Test String Potentiometers